

Power electronics contribution to renewable energy conversion addressing emission reduction: Applications, issues, and recommendations

M.A. Hannan^{a,*}, M.S. Hossain Lipu^b, Pin Jern Ker^a, R.A. Begum^c, Vasilios G. Agelidis^d, F. Blaabjerg^e

^a Department of Electrical Power Engineering, College of Engineering, Universiti Tenaga Nasional, 43000 Kajang, Malaysia

^b Centre for Integrated Systems Engineering and Advanced Technologies, Universiti Kebangsaan Malaysia, 43600 Bangi, Malaysia

^c Center for Water Cycle, Marine Environment and Disaster Management (CWMD), Kumamoto University, Kumamoto 860-8555, Japan

^d Department of Electrical Engineering, Technical University of Denmark, 2800 Kgs. Lyngby, Denmark

^e Department of Energy Technology, Aalborg University, 9220 Aalborg, Denmark

HIGHLIGHTS

- Climate change and the carbon emission is a major threat to the world.
- Converter controller offer optimal energy conversion and mitigate GHG emissions.
- Power converter technologies contribute energy conservation and improve efficiency.
- Converters are explained based on types, controls, benefits and drawbacks.
- Factors and challenges are highlighted for future converter control technologies.

ARTICLE INFO

Keywords:

Power electronics
Energy conversion
Renewable energy
Energy security
Carbon emission
Global warming

ABSTRACT

Global energy consumption is increasing at a dramatic rate and will likely continue to do so. The major source of energy is still fossil fuel, which has resulted in the well-documented problem of global warming due to the emission of greenhouse gases from the burning of such fuel. Climate change and global warming are among the crucial and complex issues encountered by the world today, and they require an immediate solution. Technological innovation is the key to ensuring energy security without causing emissions and providing efficient cost-effective energy solutions. Power electronic technologies offer high reliability and renewable energy conversion efficiency, thus contributing to energy conservation, improving energy efficiency, and helping in the mitigation of harmful global emissions. This review focuses on various aspects of power electronic technologies and their importance in tackling carbon emission and global warming problems. The key topologies of power electronic converters are explained based on types, control difficulties, benefits, and drawbacks. Power electronic controllers utilized for energy conversion are comprehensively reviewed with regard to their structure, algorithm complexity, strengths and weaknesses, and mathematical modeling. The review focuses on power converters and controllers used in different applications and highlight their contributions to energy conservation, increasing the share of renewable energy sources, and mitigating emissions. Moreover, existing research gaps, issues, and challenges are identified. The insights provided by are expected to lead to the enhanced development of advanced power electronic converters and controllers for sustainable energy conversion. Such development can reduce carbon emissions and mitigate global warming.

1. Introduction

Global energy needs continue to increase considerably due to increasing population, enhancement in the quality of life, and global industrialization [1]. Recent estimations confirm that the energy

utilization worldwide will increase by 28% between 2015 and 2040 [2]. This energy predominately originates from the burning of fossil fuel in power plants and transportation sectors; as a result, serious negative impacts, such as carbon emissions, global warming and climate change, are exerted on the environment [3,4]. Global warming

* Corresponding author.

E-mail address: hannan@uniten.edu.my (M.A. Hannan).

<https://doi.org/10.1016/j.apenergy.2019.113404>

Received 8 December 2018; Received in revised form 20 May 2019; Accepted 21 May 2019

Available online 25 May 2019

0306-2619/ © 2019 Elsevier Ltd. All rights reserved.

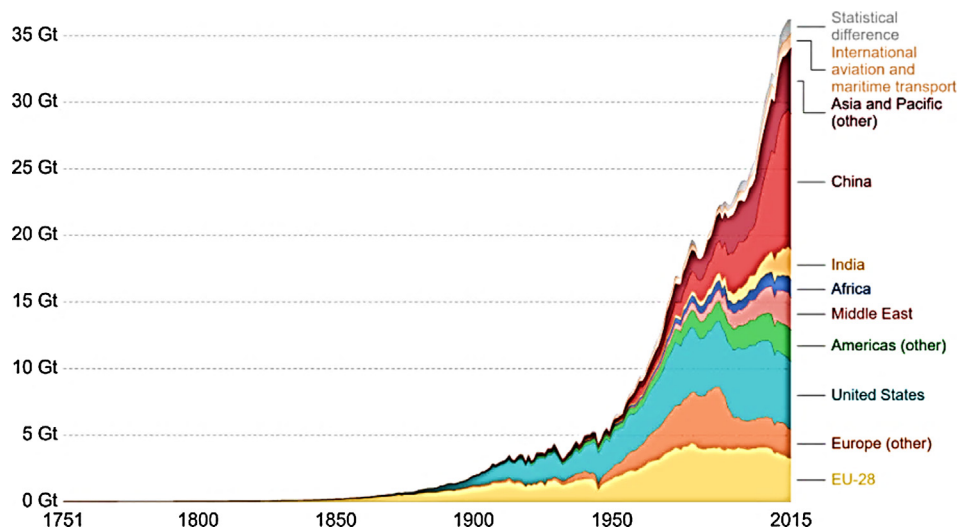


Fig. 1. Annual CO₂ emissions from fossil fuel by world region estimated in gigatons CO₂ per year (GtCO₂) [9].

poses a serious threat to human civilization due to the increase in Earth's temperature, which might disrupt the balance of the environment [5]. Science has confirmed that global warming is primarily caused by CO₂ emissions [6]. A 45% increment in the atmospheric concentration of CO₂ has been recorded [i.e., from 280 ppm in the early industrial development period (around 1750) to 405 ppm in early 2017] [7]. China and the USA are the top-ranked countries that contribute to global emission growth (28% and 15%, respectively) [8]. Fig. 1 shows the annual global CO₂ emission from fossil fuel.

Several effective approaches can be used to reduce the influence of carbon emissions and tackle global warming. One of them is to implement energy efficiency in electricity production and on the demand side [10]. Energy-efficient technologies can conserve energy and reduce environmental impacts without compromising economic advancement [11]. Energy efficiency is the fastest, most sustainable, and cost-effective means to reduce emissions and improve global energy security [12]. In addition, electricity generation using renewable energy (RE) sources, energy storage, and electrification of the transportation sector can contribute considerably to the resolution of global warming issues [13]. Reliable and environment-friendly RE sources, such as wind and solar, have reached commercial maturity and are effective solutions for decreasing global warming problems [14]. However, the performance of RE depends on enabling power electronic conversion technologies to deliver "green" and "clean" energy solutions. In addition, electrical motor drives, electric vehicles, and energy storage require power converters and appropriate controllers when used.

This work presents a review of power electronic technologies and their latest advancements and applications as key solutions in reducing the global warming effect. The review describes various converters and relevant control strategies in detail and highlights the influence of power electronic technologies on different applications. Furthermore, the review identifies existing research gaps, issues, and challenges in using power electronics to convert energy.

This study is organized into seven sections. Section 2 presents global warming causes and effects. Section 3 describes the relationship between global warming and power electronics. Section 4 introduces key power electronic converters and associated controllers and their classification, operation, strengths, and weaknesses. Section 5 discusses the potential contribution of power electronics in addressing global warming impacts. Section 6 presents the issues and challenges related to power electronic technology and provides potential recommendations to such issues. The conclusions are given in Section 7.

2. Global carbon emission: Causes and effects

Global carbon emission causes atmospheric warming. This emission results from human activities that increase the amount of greenhouse gas (GHG) contained in the atmosphere through the incomplete burning of fossil fuel. There are several factors which influence the carbon emissions such as population, industrial structure, energy intensity and economic output [15]. Global warming caused by carbon emission exerts measurable effects on the planet, such as ice melting due to increased average and extreme temperatures, extreme weather events (e.g., hurricanes and lightning), rising sea levels and ocean acidification, disturbance of Earth's ecosystems, and social effects. A detailed analysis of the causes and effects of global carbon emission is provided in the following subsections.

2.1. Potential causes of carbon emission

Several GHGs, including carbon dioxide, methane, and nitrous oxide, and a collection of a small quantity of gas make up a group called fluorinated gases ("F-gases)." Generally, the relative contribution of GHGs is considered when evaluating the global warming potential (GWP). GWP can be characterized by time ranges, and the 100-year timescale (GWP₁₀₀) is the most frequently used among all timescales. The GWP₁₀₀ metric assesses the warming influence of one molecule or unit mass of GHG relative to CO₂ in a period of 100 years [16]. The GWP₁₀₀ value of main GHGs relative to CO₂ is illustrated in Fig. 2.

CO₂ is the primary GHG expelled through daily human activities. In 2016, CO₂ accounted for 81.6% of all GHG emissions from consumers' actions in the US [18]. The actual combustion associated with fossil fuel to generate electricity and heat is the highest single source of CO₂ emissions on the planet and accounts for about 42% of complete CO₂ emissions, as shown in Fig. 3. The burning of fossil fuel, such as petrol and diesel in vehicles, was the second largest source of CO₂ emissions in

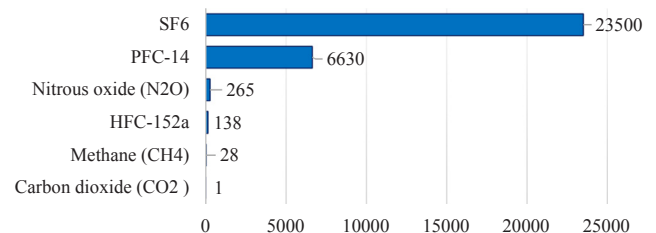


Fig. 2. GWP of GHGs over a 100-year timescale (GWP₁₀₀) [17].

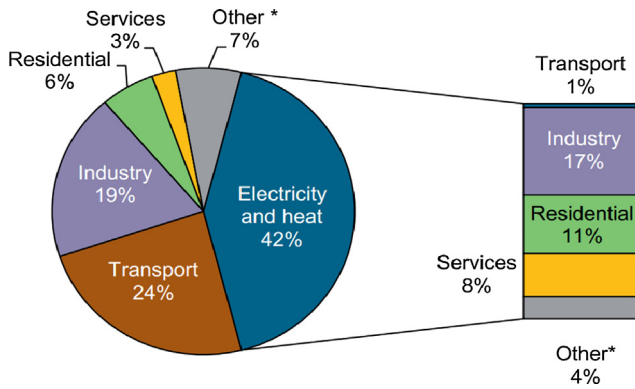


Fig. 3. Global CO₂ emissions by different sectors in 2015 [19].

2015 (24% of total CO₂ emissions) [19]. Fossil fuel ignition from diverse industrial treatments accounted for approximately 19% of all CO₂ emissions in the same year [19].

F-gases are the most powerful and most lasting type of GHGs, and their global warming impact is up to 23,000 times greater than that of CO₂ [20]. Emissions of F-gases mainly arise through gas leakage in items and products or at the end of the lifespan of products/equipment, during which F-gases are usually not fully retrieved and are damaged or reused. The four major groups of F-gases are hydrofluorocarbons (HFCs), perfluorocarbons (PFCs), sulfur hexafluoride (SF₆), and nitrogen trifluoride (NF₃). HFCs account for 85% of the existing F-gas supply [21]. Most HFCs are utilized as refrigerants in refrigerators, air-conditioning units, and heat pumps. Meanwhile, PFCs are mainly used in semiconductor manufacturing processes, and SF₆ is used in manufacturing electronics. Fig. 4 presents the emissions of F-gases. A decrease in SF₆, NF₃, and PFCs has been recorded; however, HFCs remain dominant and have been increasing gradually over the last few decades.

2.2. Carbon emission effects

IPCC AR5 Working Group III assesses the baseline scenario of emissions that have driven global warming on the basis of carbon cycle and climate modeling. Current policies are expected to limit baseline emissions from 3.1 °C to 3.7 °C warming above pre-industrial levels. A 2.6–4.0 °C warming reduction above pre-industrial levels is projected given the unconditional pledges or promises of governments. In the absence of policies, the temperature of the global environment is expected to reach 4.1–4.8 °C above pre-industrial levels. Fig. 5 illustrates the future global warming projection until 2100.

Global warming is an alarming global threat to human habitat and the environment and causes many harmful effects, such as ice melting, sea level rise, seawater acidity, droughts, heat waves, hurricanes,

tornados, heavy rains, and floods [24].

3. Relation between carbon emission and power electronics

Power electronic technologies play a vital role in efficient energy conversion and utilization, global energy conservation, environmental pollution control, and global warming reduction. A few cases prove the energy-conserving opportunities provided by power electronic systems. For instance, electricity and heat generation contribute 42% to the global emission [19]. Hence, power electronic converter-based RE systems, which involve “clean” power generation, can be utilized as a substitute for fossil fuel-based power plants. Moreover, using gasoline- and diesel-based vehicles contributes significantly to global emission. Therefore, energy storage-based electric vehicles with improved power electronic converters and associated controllers could improve performance efficiency and reduce GHG emissions. Furthermore, electrical motor drives account for 40–50% of the total consumption of global electricity, resulting in high energy costs and global emissions [25]. Hence, an efficient power electronic controller can be used to control speed, save energy, and reduce emissions. In addition, undesired harmonics in power systems lead to overheating, efficiency reduction, and low power factor and thus result in high energy consumption and carbon emission and global warming. Thus, a power electronic converter and an appropriate controller can be used to control power quality issues and reduce GHG emissions.

4. Power electronic technologies

This section explains the topologies, strengths, and weaknesses of power electronic converters. The controller structure, algorithm, and mathematical model are also presented.

4.1. Power electronic converters

Semiconductor switches are used in power electronic converters. These switches are operated at different frequencies ranging from 50 Hz to 60 Hz and even up to radio frequencies reaching 100 MHz. Power electronic converters are classified into four categories, namely, AC–DC, DC–AC, DC–DC, and AC–AC [26,27]. These converters have already been used in many applications. For instance, the AC–DC converter is used in household appliances to convert grid AC voltage to DC voltage. Grid-connected RE sources and motor drives use DC–AC converters to deliver constant/variable AC voltage. Energy storage-based devices apply DC–DC converters to achieve tightly regulated DC voltage for various loads. Furthermore, the DC–DC converter is utilized to maximize the energy of solar photovoltaic (PV) and wind turbines. AC–AC converters are suitable for altering the voltage or frequency of an AC source [28].

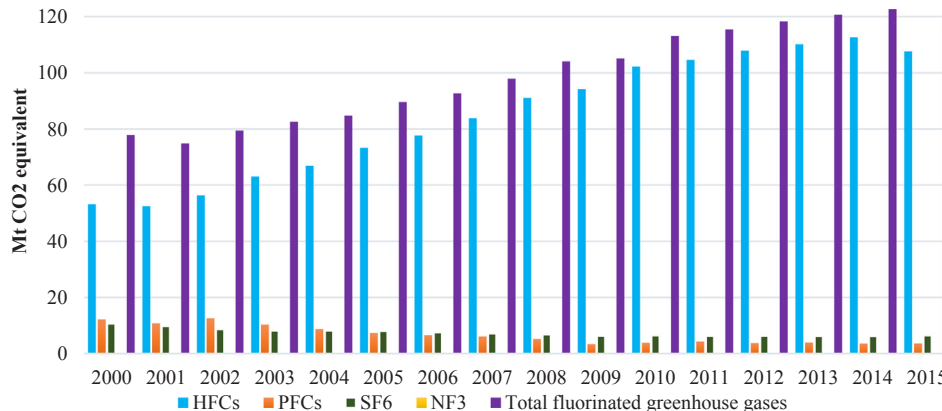


Fig. 4. Annual GHGs emissions from different F-gases in metric tons (Mt) CO₂ equivalent [22].

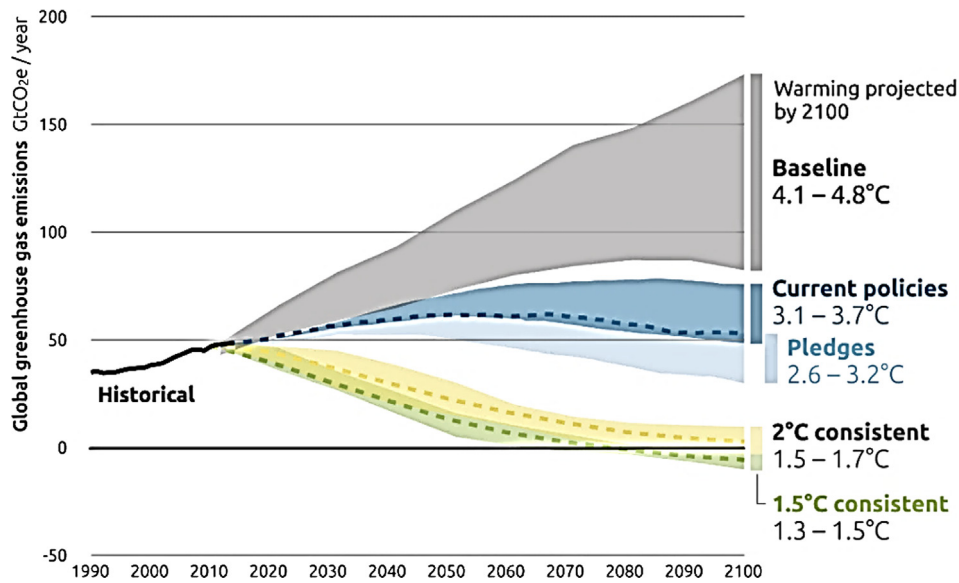


Fig. 5. Global warming projections based on pledges and current policies [23].

4.1.1. AC–DC converters

AC–DC converters are used to transform AC voltage to a steady DC output voltage. These converters can operate in low-, medium-, and high-power applications [29]. Diode rectifiers are also known as unidirectional AC–DC converters [30], and an uncontrolled rectifier consists of diodes. However, a diode rectifier results in non-negligible distortion in input current. Therefore, much effort is needed to design a filter that avoids distortion of the AC grid. Many filters should be implemented at the input because diode rectifiers cannot achieve the IEEE standard of 5% total harmonic distortion (THD) [31]. However, bulky and heavy filters could adversely affect the power factor of the circuit, thereby decreasing the efficiency of the transmission line. The development of technology in power electronics enabled the replacement of inefficient diodes by compact power factor correction (PFC) circuits, which can provide a satisfactory input signal with a unity power factor and THD under 5% [32].

Two typical PFC circuits based on harmonic compensation concepts are shown in Fig. 6. Harmonic injection could be performed either by a voltage source (Fig. 6(a)) or a current source (Fig. 6(b)). The structure of the voltage injection type is composed of a filter that comprises H-bridge configurations connected in series with an inductor [33]. This active filter compensates for the voltage ripple. However, a more

effective means to compensate harmonics for PFC is the current injection approach. Bidirectional series switches are used for current injection to the main lines. Low voltage rating, zero voltage switching performance, and low conduction losses are the advantages of this approach. The output voltage is uncontrollable in voltage and current injection compensation.

4.1.2. DC–AC converters

DC–AC converters (or inverters) deliver an AC output with a particular magnitude, phase, and frequency from a DC supply. Inverters are divided into two specific groups, namely, voltage source inverters (VSIs) [34] and current source inverters (CSIs), depending on the types of load and source [35]. The output voltage and output AC current waveforms are controlled independently in VSIs and CSIs, respectively. Buck converter topologies are employed by VSIs, whereas voltage boost inversion is adopted by CSIs. A three-phase DC–AC converter can work efficiently in medium- to high-power applications (> 5 kW), such as speed control in motors, high-voltage DC transmission (HVDC), on-grid RE sources, and numerous other industrial operations.

Three-level, three-phase inverters based on VSI and CSI topologies are shown in Fig. 7. Each topology is connected to a three-phase load via three half-bridge inverter legs. The construction of the circuit is

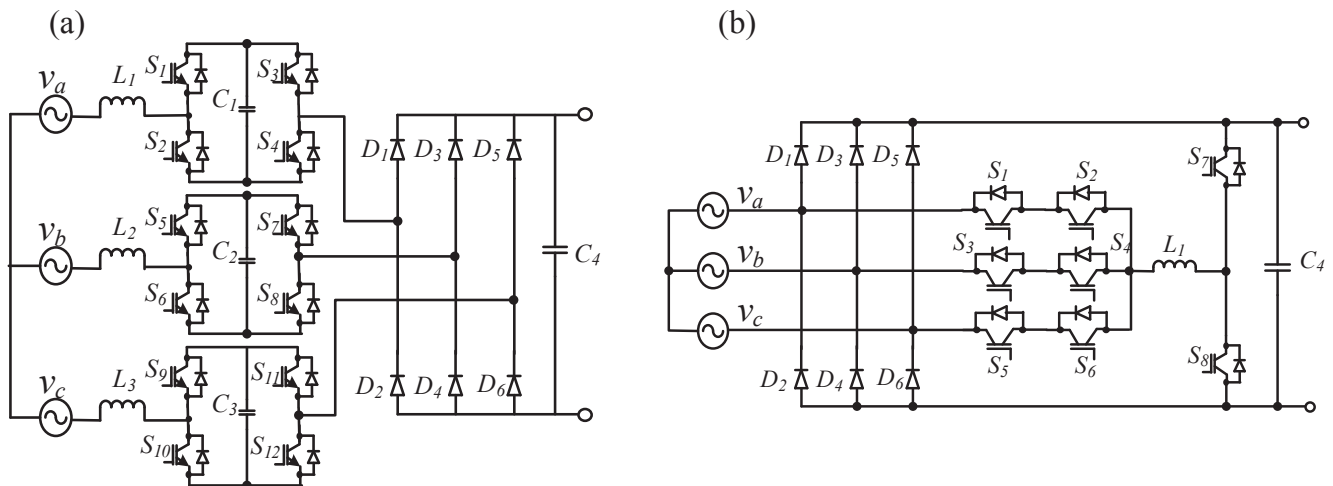


Fig. 6. PFC using harmonic compensation: (a) voltage injection method and (b) current injection method [33].

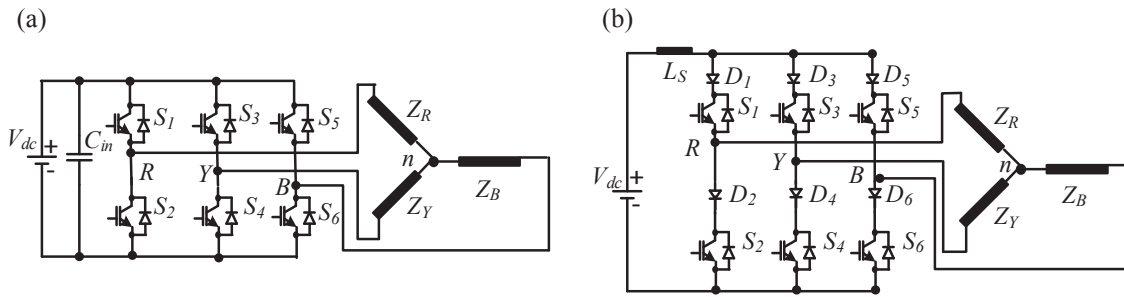


Fig. 7. Three-phase three-level inverter topologies: (a) VSI and (b) CSI [33].

identical to that of a single-phase inverter with an extra phase leg. The challenges associated with high-power-based devices can be addressed by increasing the number of phases [33]. This technique improves the power output and adds to the flexibility of regulating the inverter. A three-level line-to-line output signal with 120° out of phase can be generated with proper control techniques. The switching losses, stresses on the switching devices, harmonics, and electromagnetic interference (EMI) can be reduced using appropriate topologies, control, and modulation methods.

Numerous multilevel converter topologies with different features have been introduced in the literature [36,37]. The classification of the multilevel inverter is illustrated in Fig. 8.

4.1.2.1. Neutral point clamped topologies. Neutral-point-clamped (NPC) topologies are extensively used in high-power applications due to the low harmonic distortion and semiconductor losses. A three-level and five level diode clamped NPC (3L-DCNPC, 5L-DCNPC) topologies are shown in Fig. 9(a) and (b) respectively. Nevertheless, the diode clamped NPC has uneven power distribution losses which results in low output power capability. The three-level active neutral-point-clamped (3L-ANPC) has addressed the drawbacks of DLNPC by replacing the clamping diodes with antiparallel diodes in order to deliver a controllable path for the neutral current. The different topologies of active neutral-point-clamped (5L-ANPC, 7L-ANPC, 9L-ANPC, ...) are employed in various application such as pumps, fans, tractions and rolling mills and semiconductor technology, as shown in Fig. 9(c) and (d) [38,39].

4.1.2.2. Multicell multilevel inverter topologies. Multilevel inverter topologies use different configurations of basic power-cell to meet the requirement of output voltage levels as presented in Fig. 10. The Cascaded H-Bridge (CHB) is designed using isolated power supply for each basic cell, whereas multilevel modular converter (MMC) and Flying Capacitor (FL) are configured using a common shared voltage source. The multicell multilevel topologies have the advantage of having modular design which exhibits low maintenance cost. Nonetheless, they need active and passive components together with additional components and improved control techniques to balance the

voltage in the capacitor [40,41].

4.1.3. DC-DC converters

DC-DC converters receive DC input voltage and convert it to DC output voltage at a higher or lower level, and in several cases, at a different polarity. These converters can control the output voltage and load deviation. DC-DC converters can provide variable DC voltage to regulate the motor speed. The pulse width modulation (PWM) control method is used to control the output voltage by adjusting the switch ON time. On the basis of the application's requirement, complex structures can be constructed using coupling inductors and/or transformers between the input and output [42,43]. DC-DC converters can be categorized into two groups such as non-isolated DC-DC converters and isolated DC-DC converters [33].

4.1.3.1. Non-isolated DC-DC converters. The Non-isolated DC-DC converters are built using an inductor/couple of inductor, a capacitor, a switch, and a diode, as displayed in Fig. 11. These converters have magnetic storage feature which makes them heavy and bulky. Besides, they have low efficiency and low power density. These converters are functioned either using continuous conduction mode (CCM) or discontinuous conduction mode (DCM). Due to the low efficiency, high-current ripple and load dependent voltage gain of DCM operation, CCM operation is dominant in different operations. However, DCM operation is suitable where the fast dynamic response is preferred [44]. Non-isolated DC-DC converters can be broadly classified as step-down, step-up, and step-up-down, which are described in the following subsection [45].

• Buck converter

A buck converter is a step-down converter that generates an output voltage that is lower than the input voltage. This converter is operated using two continuous conduction mode (CCM) operations: switch ON and OFF states. When the switch is turned OFF, the diode operates as a freewheeling diode, and the load current passes through it. When the switch is turned ON, the output voltage is regulated [46,47].

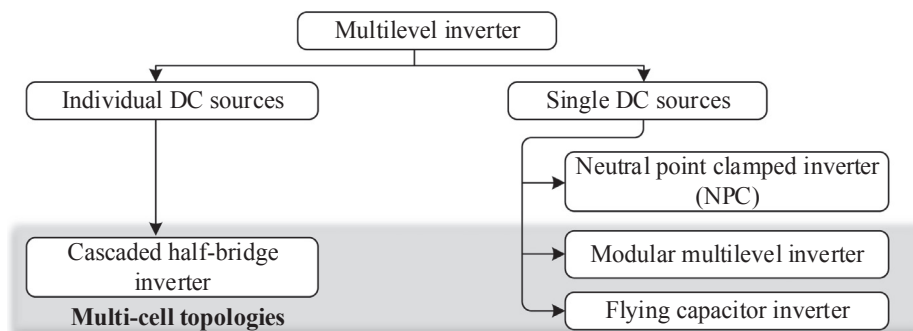


Fig. 8. Classification of multilevel inverter.

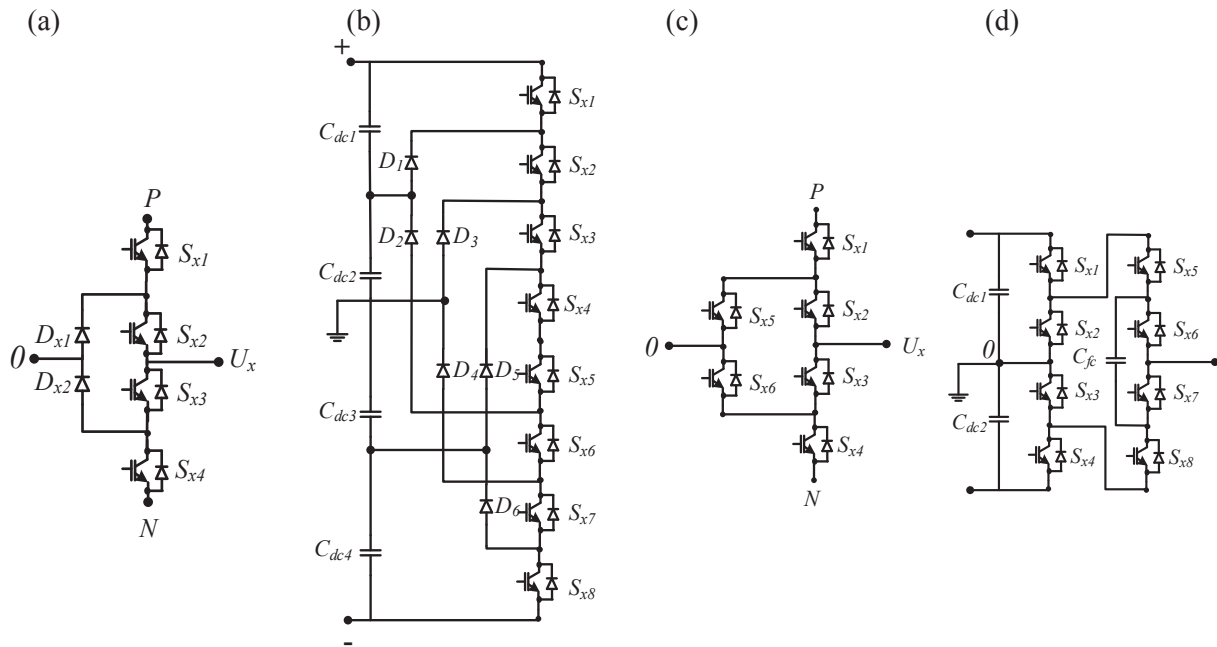


Fig. 9. NPC inverter topologies (a) 3L DCNPC (b) 5L DCNPC (c) 3L ANPC (d) 5L ANPC [33].

• Boost converter

A boost converter is a step-up converter that produces an output voltage that is higher than the input voltage. Possessing the same characteristics as the buck converter, the boost converter has two main states: ON and OFF. The input voltage is on the inductor during the ON condition of the switch, and it is on the diode during the OFF state. Hence, the output voltage is similar to the addition of the input voltage to a ratio of the input voltage. A boost converter has a right half plane zero in its control to output a transfer function because of the input inductor, which makes the operation of closed-loop control a challenging task [48,49].

• Buck-boost converter

A buck-boost converter can operate either as step-down or step-up converter. The converter acts like a buck converter when the duty cycle is below 0.5. However, the converter works as a boost converter when the duty cycle is tuned between 0.5 and 1. This type of converter is appropriate when a large variation in input voltage is observed and buck and boost converter operations are required [50,51].

• Cuk converter

A Cuk converter is constructed using a step-down-up converter with an inverting output. It uses a capacitor for energy storage instead of an inductor. A Cuk converter has advantages over a buck-boost converter. The first one is the grounded source switch configuration that helps a Cuk converter simplify and facilitate its drive circuit. Another advantage is its operation as an isolated state that can be configured using an additional capacitor and an AC transformer. In addition, low output ripple can be obtained by coupling the two discrete inductors on a single core. Hence, size and cost are minimized. Moreover, a Cuk converter can provide multiple DC outputs by employing multiple secondary winding transformers [52,53].

• SEPIC converter

The single-ended primary inductor converter (SEPIC) is designed using a step-down-up converter and non-inverting output with only one grounded switch. It changes the voltage level by transferring energy between the inductors and capacitor; therefore, a high-current capacity-based capacitor is required. Similar to a buck-boost converter, SEPIC has a pulsating output current wave shape. SEPIC's inductors can also

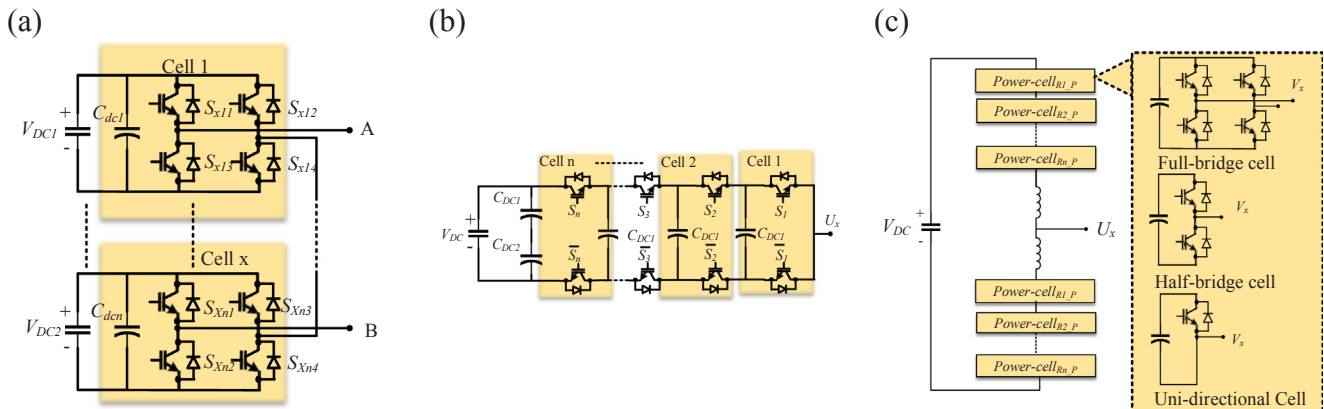


Fig. 10. Multilevel inverter topologies (a) CHB (b) FL, (c) MMC [33].

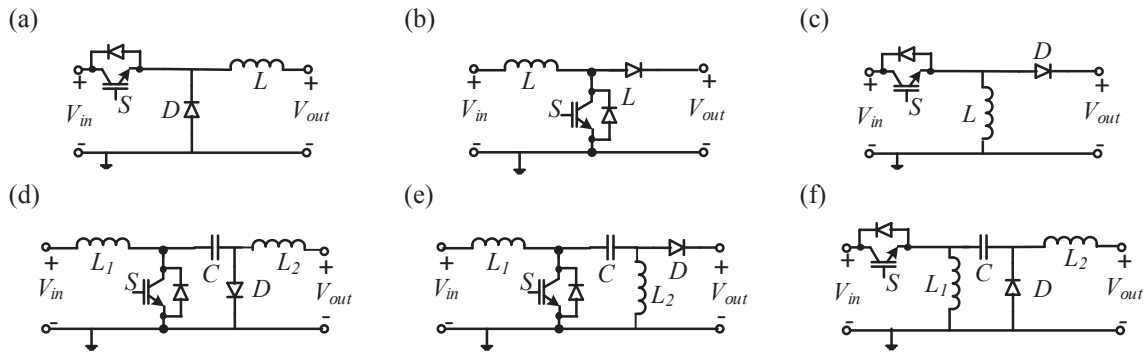


Fig. 11. Various fundamental non-isolated DC-DC converters: (a) buck, (b) boost, (c) buck-boost, (d) Cuk, (e) SEPIC, and (f) Zeta [33].

be paired to build an isolated DC-DC converter [54,55].

• Zeta converter

The Zeta converter can step-down and step-up the output voltage level. This converter operates in a similar manner as SEPIC does and generates a positive voltage wave shape from the input voltage. The Zeta converter needs extra components because its topology is based on the buck converter, and it has a floated switch. Contrary to the Cuk converter, the Zeta converter has a pulsating-shaped input current. This converter is often described as dual SEPIC [56,57]. Fig. 11 and Table 1 show the configuration and performance characteristics of all non-isolated DC-DC converters.

4.1.3.2. Isolated DC-DC converter. Electrical isolation in DC-DC converters is structured using either transformer or coupled inductor. They can provide satisfactory results by reducing noise and electromagnetic interference (EMI) [44]. Such converters are operated at high frequency where energy is stored in coupled inductor in one cycle which is transferred to the load in the other cycles. The well-known isolated DC-DC converters topologies are shown in Fig. 12.

• Flyback Converter

Flyback DC-DC converters is formed using a coupled inductor rather than an isolation AC transformer as presented in Fig. 12(a). The working principle of flyback converter is similar to buck-boost DC-DC converter where energy is stored when the switch is turned ON and then energy is transferred to the load when the switch is turned OFF. This converter can deliver different results by tapping the secondary winding of the coupled inductor and is appropriate for low power applications (< 100 W) [58].

• Forward Converter

Forward DC-DC converter is a type of buck converter which is built using AC transformer without air gap as shown in Fig. 12(b). This

converter can deliver energy directly without storage while the switch is functioned in ON state. The different voltage level of this converter can be obtained by changing the transformer turns ratio. This converter operates satisfactorily in medium power applications (200–500 W) [59].

• Push-Pull Converter

Push-Pull DC-DC converter is configured using the two switches at the primary side of the transformer, as illustrated in Fig. 12(c). The transformer of this converter has bidirectional excitation. This converter features low noise and steady current flow [60].

• Half-Bridge Converter

Half-bridge DC-DC converter is designed using two switches which are turned on alternatively to excite the transformer, as shown in Fig. 12(d). The input voltage of this converter can be divided using two capacitors located at the primary side of the transformer. This converter has low switch voltage stress and is usually used in application up to 500 W [61].

• Full-Bridge Converter

Full-bridge DC-DC converter is structured using four switches operated symmetrically at the primary side of the transformer, as shown in Fig. 12(e). This converter operates like buck converter for voltage conversion. This converter is appropriate for applications in kW range [62].

4.1.4. AC-AC converters

AC-ACs converters are widely used in industrial applications where AC load output voltage is required with different amplitudes, phases, and frequencies. A standard AC-AC converter is formed by using a rectifier and an inverter with a DC link voltage placed in between.

4.1.4.1. Cycloconverter. The cycloconverter is the most commonly used frequency changer, where AC power from a specific frequency is

Table 1 Characteristics of various non-isolated DC-DC converters.

Type of converter	Buck converter	Boost converter	Buck-boost converter	Cuk converter	SEPIC converter	Zeta converter
Switching time	Very high	Very high	Very high	High	High	Medium
Execution difficulty	Difficult	Difficult	Difficult	Medium	Difficult	Difficult
Control difficulty	Complex	Complex	Complex	Complex	Complex	Complex
Power loss	Negligible	Negligible	Negligible	Quite low	Low	Low
Size	Small	Small	Medium	Medium	Small	Medium
Voltage/current stress	Low/low	Low/low	Low/low	Low/low	Low/low	Low/low
Efficiency	Excellent	Excellent	Excellent	Excellent	Excellent	Excellent
Cost	Low	Medium	Medium	Medium	Low	Medium

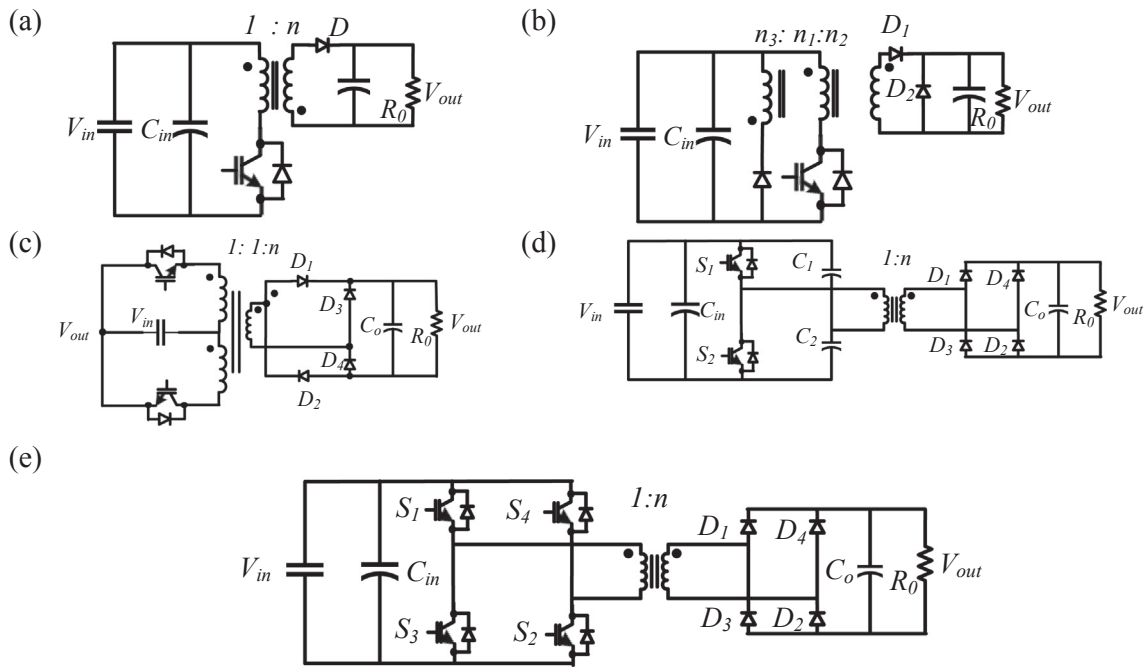


Fig. 12. Isolated DC-DC converter (a) flyback converter, (b) forward converter, (c) push-pull converter, (d) half-bridge converter, and (e) full-bridge converter [33].

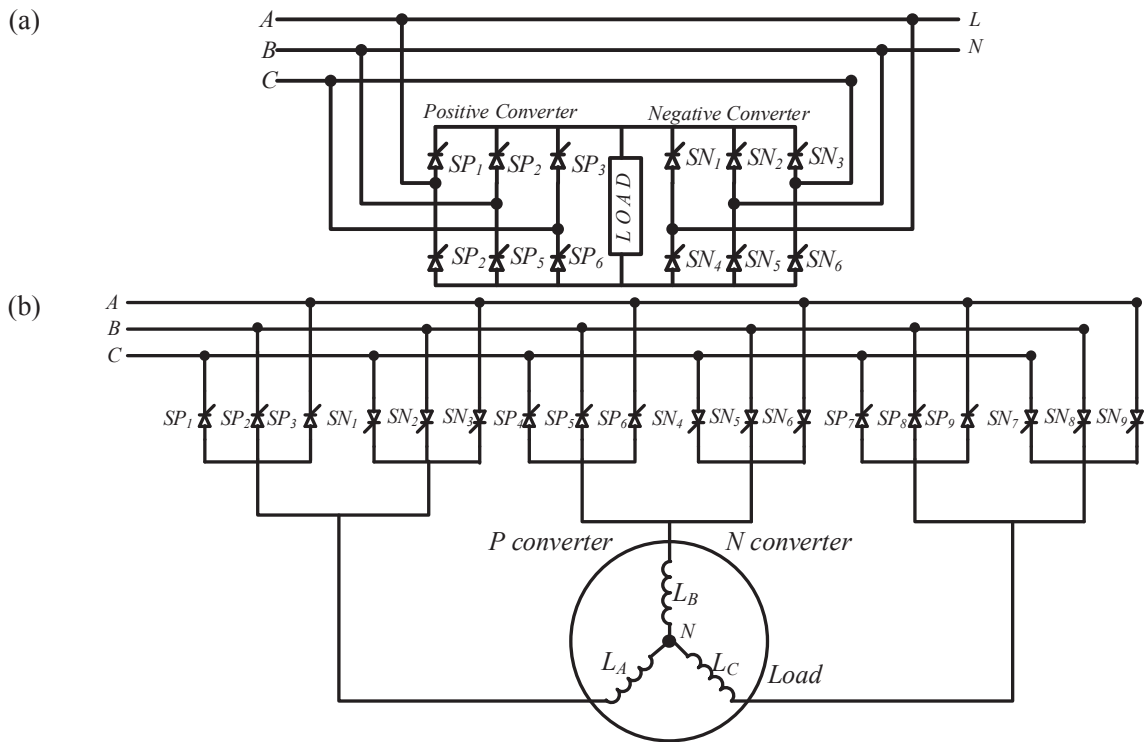


Fig. 13. Configuration of (a) single-phase bridge cycloconverter and (b) three-phase half-wave cycloconverter [33].

changed to a different frequency without the need for any intermediate DC link [63]. The structure of a cycloconverter consists of a half-wave or full-wave bridge. The configuration is built using back-to-back connected-controlled rectifiers. The frequency and voltage in the output signal can be regulated independently and consistently by adjusting the firing angles of the controlled rectifiers [64]. A single-phase bridge cycloconverter configuration is shown in Fig. 13(a). The configuration includes two back-to-back connected rectifiers and positive (P-type) and negative (N-type) converters. This type of cycloconverter is extensively employed in electric traction

applications. Fig. 13(b) shows the configuration of a three-phase, half-wave cycloconverter. Its structure is similar to that of a single-phase cycloconverter, where P-type and N-type converters conduct positive and negative currents, respectively. This kind of cycloconverter is applied in high-capacity motor drives. Cycloconverters use a high number of pulses (6-pulse, 12-pulse, etc.) to decrease oscillation and achieve a smooth output [65].

4.1.4.2. Matrix converter. Matrix converters are designed using bi-directional switches without DC-link voltage, as shown in Fig. 14.

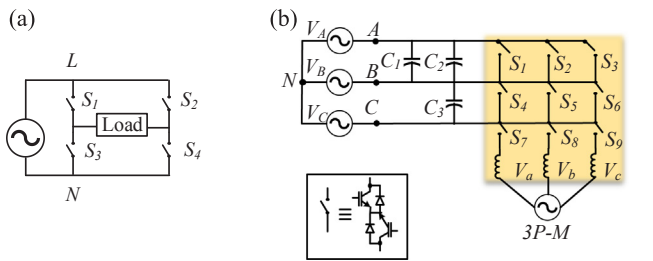


Fig. 14. Matrix converter structures, (a) 2 × 2 matrix converter (b) 3 × 3 matrix converter [33].

Matrix converter exhibits simple, compact structure and has unity power factor and can deliver reliable power flow with sinusoidal waveform. The matrix converter is usually voltage-fed at the input and hence should not be short circuited and they are usually inductive at the load side and therefore should not be open circuited [66]. Fig. 14(a) presents the structure of 22 matrix converter which has stepped-down amplitude and stepped-up frequency harmonics. Moreover, this converter has instantaneous maximum output voltage similar to the maximum value of the input voltage. A layout of 33 matrix converter is illustrated in Fig. 14(b) where 27 switching states can be generated by connecting three-phase input source to the each phase of the load [66]. Table 2 shows the performance comparison of different converters.

4.2. Power electronic controller in energy conservation

Power electronic control schemes have been used in numerous applications. The function of a controller is to regulate the main variables, such as voltage, current, speed, torque, and rotor flux, to achieve high performance and efficiency and consequently cut off emissions. Controllers can be classified as conventional or intelligent. The conventional controller is widely used as a control technique for several scalar [67] and vector controllers [68]. The intelligent controller is used to adjust control parameters online on the basis of adaptive modeling with sudden changes in systems. The intelligent controller has several advantages over the conventional controller; for example, it does not require a mathematical model, and it can handle linear and nonlinear systems.

4.2.1. Conventional controller

Proportional integral (PI), proportional derivative (PD), and PI derivative (PID) controllers are distinct categories of conventional controllers that regulate speed, torque, current, and voltage. Among them, the PID controller is regarded as the best due to its effective control strategy [69]. The PID controller has several advantageous features, such as cost competitiveness and simple construction and design, and it

Table 2
Performance comparison of different converters.

Type of converter	Strength	Weakness	Application
AC-DC	<ul style="list-style-type: none"> ● Low voltage rating ● Zero voltage switching performance ● Low conduction loss 	<ul style="list-style-type: none"> ● Limited power supply ● High harmonics distortion 	Household appliances, cellular phones, laptops
DC-AC	<ul style="list-style-type: none"> ● Low switching losses ● Low stress ● Low harmonics 	<ul style="list-style-type: none"> ● Low power factor ● Complex circuit 	Solar PV, wind
DC-DC	<ul style="list-style-type: none"> ● Fast dynamic response ● High efficiency ● Low cost ● Low noise 	<ul style="list-style-type: none"> ● High conversion loss ● High cost ● Large size ● Switching losses 	Electric vehicles, trolley cars
AC-AC	<ul style="list-style-type: none"> ● High efficiency ● Less maintenance ● Controlled flexibility 	<ul style="list-style-type: none"> ● Large size ● High harmonics 	Electric traction, high-capacity motor

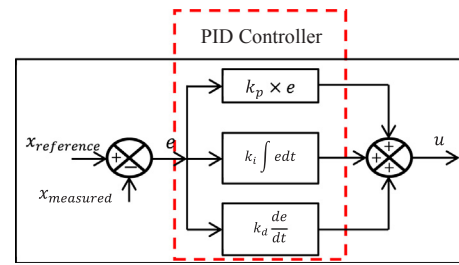


Fig 15. Structure of PID control.

is extensively used in industries to regulate motor speed [70,71]. Fig. 15 shows the structure of the PID controller. The structure is built by using measured and reference values to calculate the error signal (error in speed, torque, flux, current, or voltage) for controlling signals.

The sum of errors is achieved at the output signal of the PID controller, and it consists of proportional, integral, and derivative errors, as shown in the equation below.

$$u(t) = K_p e(t) + K_i \int_0^t e(t) dt + K_d \frac{de(t)}{dt}, \quad (1)$$

where e is the error, $e = (x_{reference} - x_{measured})$; u represents the output signal; and K_p , K_i , K_d denote the proportional, integral, and derivative gains, respectively. The PID controller's efficiency depends primarily on PID parameters. Appropriate value of K_p , K_i , and K_d will enhance the overall performance of the system. Each parameter has several salient features and plays a vital role in controlling the variables, as presented in Table 3.

Although the PID controller has an easy construction, it has many weak points, such as vulnerability to temperature and model parameter variations. In addition, the model requires numerical calculation and has a rapid response to load disturbances. Moreover, selection of appropriate variables to enhance steadiness is a time-consuming process [72]. Hence, investigations have been performed to determine suitable PID parameters. The produced methods include Ziegler–Nichols, lambda tuning, Cohen–Coon [73,74], and visual loop tuning methods. However, these methods use the inefficient trial-and-error method, have a mathematical model, and entail complex calculation operations. Thus, a number of optimization algorithms have been introduced to search for the optimal parameters of PID controllers [75].

4.2.2. Intelligent controllers

Intelligent controllers have become popular in recent years because they are robust and possess the computational capability to control complex systems. The benefits of using intelligent controllers are as follows. First, their structure does not need a mathematical model. Second, they perform well when correctly tuned. Third, they can be customized using linguistic information obtainable from specialists or

Table 3
Characteristics of PID control parameters.

Type	Rise time	Overshoot	Settling time	Steady-state error
K_p	Decrease	Increase	Small change	Decrease
K_i	Decrease	Increase	Increase	Eliminate
K_d	Minor change	Decrease	Decrease	No effect

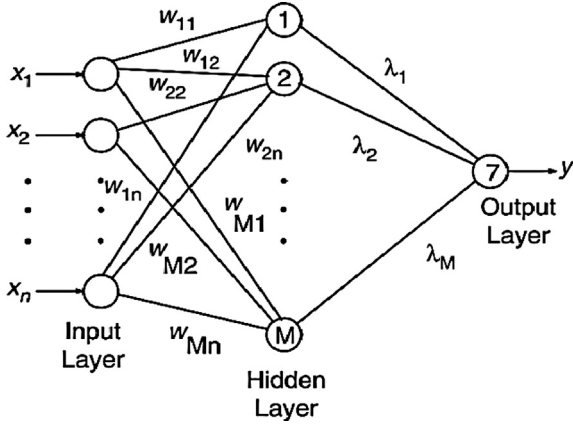


Fig. 16. Architecture of ANN [78].

by using clustering or other approaches. Fourth, they require less adjustment than conventional controllers. (V) They may be constructed using real data without the need of experience. Lastly, they can be designed based on a combination of response and linguistic-based information [76].

4.2.2.1. Artificial neural network (ANN) controller. Artificial intelligence (AI)-based controllers have been used in various applications. ANN uses biological neural networks that consist of information control processes with several common performance properties [77]. ANN has an intelligent algorithm which consists of three layers, such as, the input layer, hidden layer, and output layers, as presented in Fig. 16. Each layer consists of a number of neurons or nodes with activation functions.

Consider the input layer includes n inputs and hidden layer consists of M hidden nodes. The input n variables (n inputs) are represented as $x_1, x_2, x_3, \dots, x_n$. The node (neuron) is composed of two segments which are net function and activation function. A function $y = f(x_1, x_2, x_3, \dots, x_n)$ is to be approximated, and the approximator uses the sum of nonlinear functions $g_1, g_2, g_3, \dots, g_{2n+1}$, where each g represents the nonlinear functions of a single variable. Therefore,

$$y = f(x_1, x_2, x_3, \dots, x_n) = g_1 + g_2 + g_3 + \dots + g_{2n+1} = \sum_{i=1}^{2n+1} g_i, \quad (2)$$

where g_i denotes a real and continuous nonlinear function. The output y can also be expressed as

$$y = \sum_{j=1}^n w_{ij}x_j = w_{i1}x_1 + w_{i2}x_2 + \dots + w_{i3}x_n \quad (3)$$

where w_{ij} is the weights between the input and hidden layers.

Three kinds of activation function are employed in ANN network that are sigmoid, tansigmoid, and purelin activation function, as presented in Fig. 17. One of the most widely used training techniques is back-propagation (BP). The training process of the BP network includes three phases: data training algorithm execution, associated error estimation, and weight adjustment [79].

The output of a single neuron can be presented as

$$a_i = f_i \left\{ \sum_{j=1}^n w_{ij}x_{ij}(t) + b_i \right\}, \quad (4)$$

where f_i is the activation function and b_i is the bias.

The training method of ANN begins with the input and output data and weight configuration. Subsequently, data training is performed by providing real input data. Then, ANN delivers the necessary output data. The total network error (sum of squared errors) is obtained as

$$E = \frac{1}{2} \sum_{k=1}^P \sum_{j=1}^K (d_{kj} - O_{kj})^2, \quad (5)$$

where E stands for the total error, P represents the number of patterns in the training data, k is the number of outputs in the network, d_{kj} denotes the target output for pattern K , and O_{kj} indicates the j th output of the k th pattern. The network error can be reduced by choosing an appropriate training algorithm. Common training algorithms include Levenberg-Marquardt, gradient descent with momentum, reduced memory, and Bayesian regularization [80].

4.2.2.2. Fuzzy logic controller. Fuzzy logic controller (FLC) is another prominent controller used extensively in motor drives. FLC has been discussed in many technical articles due to its easy execution, absence of any mathematical relationship, and capability to work efficiently in linear and nonlinear systems using linguistic rules. FLC is superior to other controllers because of its robust control capability and quick response to a transient condition [81]. However, the effectiveness of FLC depends on the type of MFs, number of rules, and rule base.

FLC is designed based on four steps, namely, fuzzification, rule base, inference engine, and defuzzification. Fuzzification investigates every input into a group with convenient linguistic values, as shown in Fig. 18.

(i) Definition of module characteristics

The first step of FLC involves the number of inputs, outputs, and position of fuzzy MFs based on knowledge. The input data include an error (e) and a change in error (de), which are expressed as

$$e(t) = x_n^* - x_n, \quad (6)$$

$$de(t) = e(t) - e(t-1). \quad (7)$$

(ii) Fuzzification design

Fuzzification can be performed using any number of normalizing expressions. Linear and Gaussian are two well-known functions in fuzzification design [4], and they are expressed mathematically in Eqs. (8) and (9), respectively. The two expressions have common parameters. The midpoint and width in the linear function are specified by σ_L and μ_L , respectively. Similarly, in the Gaussian function, the width and midpoint are represented by μ_G and σ_G , respectively.

$$\text{Linear function: } \begin{cases} 1 - \left| \frac{x - \mu_L}{\sigma_L} \right| & \text{if } x \in [(\mu_L - \sigma_L), (\mu_L + \sigma_L)] \\ 0 & \text{Otherwise} \end{cases} \quad (8)$$

$$\text{Gaussian function: } \exp\left(-\frac{(x - \mu_G)^2}{2(\sigma_G)^2}\right) \quad (9)$$

where

$$\mu_L = \mu_G \quad (10)$$

$$\sigma_L = 3\sigma_G \quad (11)$$

Consider linguistic variable x and three fuzzy variables, namely, positive (PV), zero (ZE), and negative (NV). If the membership function (fuzzifier) is denoted by X , then the three membership functions (MFs) are XPV, XZE, and XNV. U_x signifies the fuzzy linguistic universe for

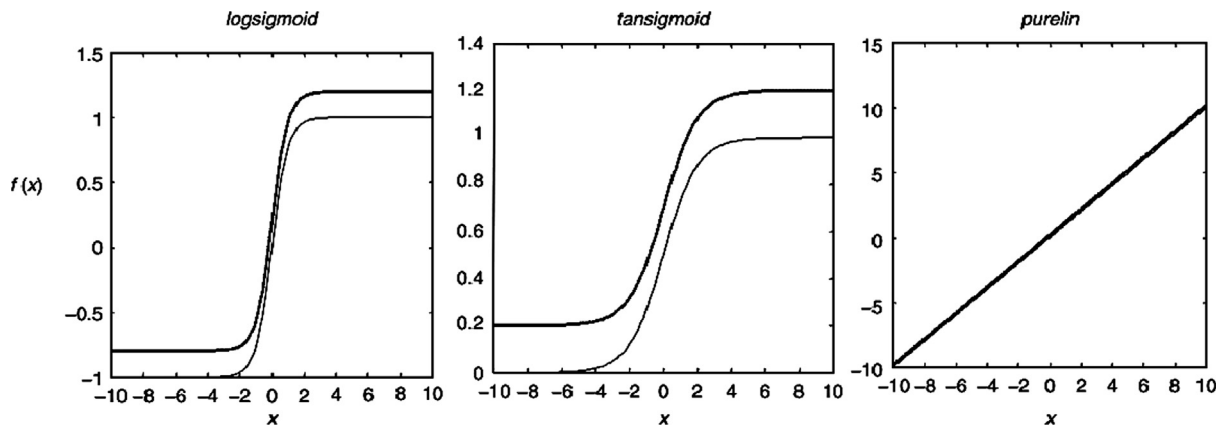


Fig. 17. Logsigmoid, tansigmoid, and purelin activation functions [78].

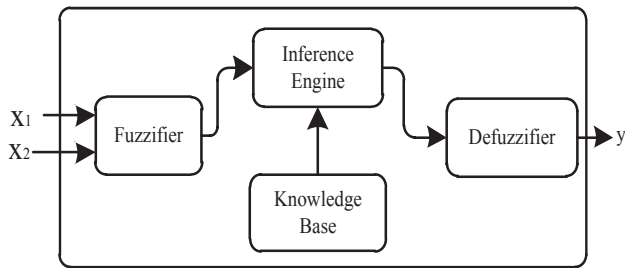


Fig. 18. Structure of a fuzzy logic controller.

input x and is shown in the following equation.

$$U_x = [X_{NV} X_{ZE} X_{PV}], \quad (12)$$

where X_{PV} is the membership function for the positive fuzzy variables, X_{ZE} is the membership function for the zero fuzzy variables, and X_{NV} is the membership function for the negative fuzzy variables.

A different form of MF based on Eqs. (8)–(11) is shown in Fig. 19. FLC performance will improve if the MFs are selected accurately. Conventional FLC uses the trial and error method to determine MFs. However, this method is unreasonable due to its complex mathematical

computations, and much time and effort are required to find the solution [82].

(iii) Interference engine design

The third stage of FLC uses control rules and linguistic terms for decision making. Inference systems are typically grouped into two categories, namely, Mamdani and Takagi-Sugeno. The Mamdani method is commonly used because of its simple design and easy construction. The fuzzy rule is represented as an “if-then” rule. The output MFs associated with the inputs (e, de) and the output (ω_{sl}) are operated by the fuzzy rule [83]. The rules are shown in the subsequent equations, and Table 4 presents the information of the 49 rules.

-
- Rule 1: If e is “Ne3” and de is “Nde3,” THEN u is “NB.”
 - Rule 2: If e is “Ne3” and de is “Nde2,” THEN u is “NB.”
 -
 - Rule 48: If e is “Pe2” and de is “Pde3,” THEN u is “PB.”
 - Rule 49: If e is “Pe3” and de is “Pde3,” THEN u is “PB.”
-

(iv) Defuzzification design

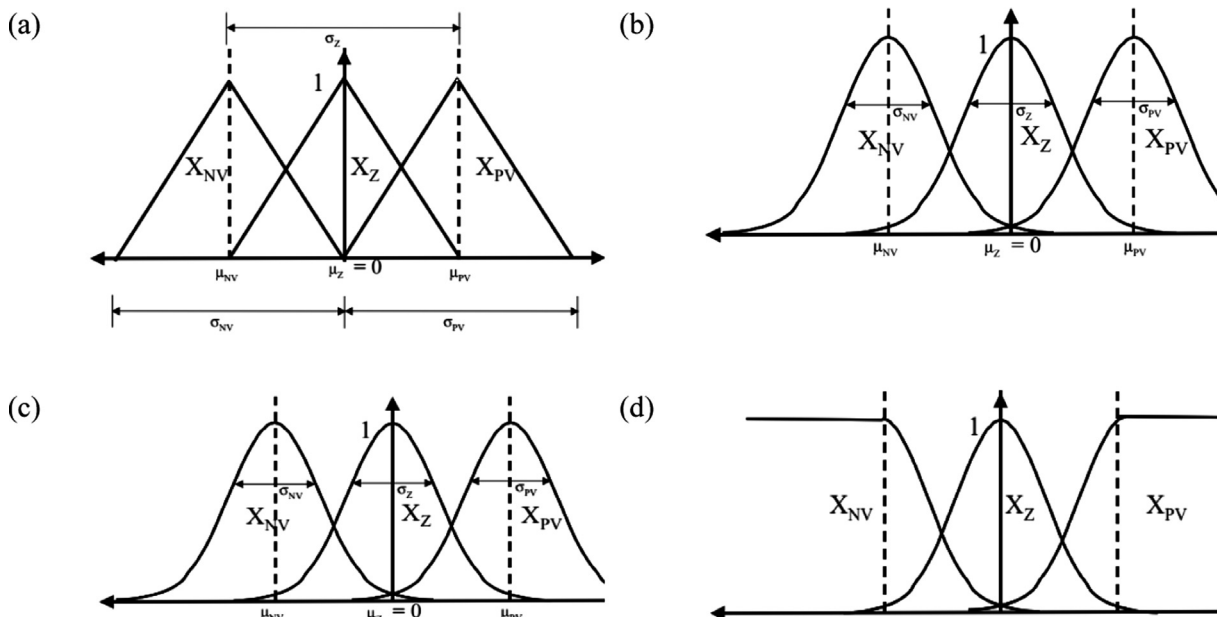


Fig. 19. (a) Fuzzy linear membership functions, (b) linear-trapezoidal membership functions, (c) Gaussian membership functions, and (d) Gaussian-trapezoidal membership functions [76].

Table 4
Fuzzy rules for interference engine design in fuzzy logic system.

de	e						
	Ne3	Ne2	Ne1	Ze	Pe1	Pe2	Pe3
Nde3	NB	NB	NB	NB	NM	NS	Z
Nde2	NB	NB	NB	NM	NS	Z	PS
Nde1	NB	NB	NM	NS	Z	PS	PM
Zde	NB	NM	NS	Z	PS	PM	PB
Pde1	NM	NS	Z	PS	PM	PB	PB
Pde2	NS	Z	PS	PM	PB	PB	PB
Pde3	Z	PS	PM	PB	PB	PB	PB

NB: Negative big; NM: Negative medium; NS: Negative small; Z: Zero; PS: Positive small; PM: Positive medium; PB: Positive big.

The final step of FLC is defuzzification. In this stage, FLC provides the output values as a crisp value. Moreover, this process performs some adjustment and controls the crisp value of the output MFs. Control and adjustment of the crisp value in output MFs are executed in this stage. However, these MFs are needed to select the number of MFs and related boundaries. The trial-and-error approach is utilized to find the optimal value of MFs [84].

$$O_{crisp} = \frac{\sum_i^n w_i \cdot u_i}{\sum_i^n w_i} \tag{13}$$

where n denotes the number of rules, u indicates the value of output MFs, and w represents the weight coefficient. The weights are assessed using the minimum value between $\mu_e(e)$ and $\mu_{de}(de)$, as shown in the equation

$$w_i = \min[\mu_e(e), \mu_{de}(de)] \tag{14}$$

4.2.2.3. ANFIS controller. Combining fuzzy logic and neural network generates a new method called the adaptive neuro fuzzy interface system (ANFIS), which inherits the benefits from the various properties of the two combined concepts. ANFIS has become popular in estimating different parameters because it does not require a mathematical model and has an excellent capability to control any sudden change in speed or load [85]. However, ANFIS has a few drawbacks, such as its complex computation and requirement for substantial data to be used for data training and learning [86]. The typical rule set of ANFIS is generated using a number of inputs (x_1, x_2, \dots, x_n) with the first-order Takagi–Sugeno fuzzy model and a function response of f_1, f_2, \dots, f_n . It can be expressed in the following form [87].

Rule 1: If x_1 is A_1 and x_2 is B_1 , then $f_1 = p_1 x_1 + q_1 x_2 + r_1$.
 ...
 Rule n : If x_n is A_n and x_n is B_n , then $f_n = p_n x_n + q_n x_n + r_n$.

The MFs for inputs (x_1, x_2, \dots, x_n) are represented by the nonlinear parameters A_i, B_i , and linear activation functions are denoted by p_i, q_i, r_i . The structure of the ANFIS architecture includes five layers, namely, layer 1 (input layer), layer 2 (input membership function), layer 3 (rule layer), layer 4 (output membership function), and layer 5 (defuzzification layer). Each input is connected with MFs. Fig. 20 shows an ANFIS structure built with two inputs.

Layer 1: Input layer

Each node in this layer corresponds to an input variable. The input variables are represented by voltage error $e(k) = V_0(k) - V_{0ref}(k)$ and change in voltage error $\Delta e(k) = [e(k) - e(k - 1)]$. The fuzzy sets are configured using positive large (PL), positive medium (PM), positive small (PS), and small (S) for the input variable voltage error $e(k)$ and by using positive medium (PM), zero (ZE), and negative medium (NM) for

the change in voltage error $\Delta e(k)$.

The output of neuron i in layer 1 is obtained as

$$O_i^1 = f_i^1(net_i^1) = net_i^1, \tag{15}$$

where net_i^1 denotes the error and the change in the error of the i th input of layer 1.

Layer 2: Input membership function

The MF of an input value belonging to a fuzzy set is determined in this layer. The output of the second layer for neuron j using triangular MF can be achieved as follows:

$$O_j^2 = f_j^2(net_j^2) = \frac{(X_i - a_j)}{(b_i - a_j)}, \tag{16}$$

where X_i represents the i th input variable to the node of layer 2 and a_j is the j th membership function corners in layer 2.

Layer 3: Rule layer

Each node in layer 3 calculates the output by multiplying the incoming signal. An input node belongs to A1–A4 MF nodes representing the voltage error, whereas the other input node belongs to B1–B3 MF nodes representing the change in voltage error in layer 2. Accordingly, the fuzzy rule set is formed using 12 nodes in layer 3.

The outcome is the strength applied to the evaluation of the effect defined for each particular rule. The output in layer 3 for neuron k is

$$O_k^3 = f_k^3(net_k^3) \text{ where } net_k^3 = \prod_j w_{jk}^3 y_j^3, \tag{17}$$

where y_j^3 represents the j th input to the node of layer 3 and w_{jk}^3 is assumed to be infinite.

Layer 4: Output membership function

This layer evaluates the output by taking the output of layer 3 multiplied by the connecting weights, which is expressed as

$$O_m^4 = f_m^4(net_{km}^4) = \max(net_{km}^4), \tag{18}$$

$$net_{km}^4 = O_k^3 w_{km}. \tag{19}$$

Count k denotes the links from layer 3 to the specific m th output in layer 4, and w_{km} represents the link weight associated with the k th rule.

Layer 5: Defuzzification layer

The output of ANFIS is achieved in layer 5, which is known as the defuzzification layer. A crisp fuzzy output is formed by taking output fuzzy sets combined with the single fuzzy set, as expressed in the following equations.

$$O_o = f_o^5(net_o^5), \tag{20}$$

$$net_o^5 = \frac{(\sum_m o_m^4 a_{cm} b_{cm})}{\sum_m (a_{cm} b_{cm})}, \tag{21}$$

where a_{cm} and b_{cm} represent the center and width of the output fuzzy sets, respectively.

The hybrid algorithm has been proven effective in achieving good learning and training of ANFIS [88]. The hybrid algorithm includes forward and backward pass functions. Least square estimation (LSE) is utilized as a forward pass to optimize the consequent parameters (p_n, q_n, r_n), and gradient descent BP is adopted as a backward pass to obtain the optimal solutions of the premise parameters (a_n, b_n, c_n). Table 5 shows the comparative performance of different controller technologies.

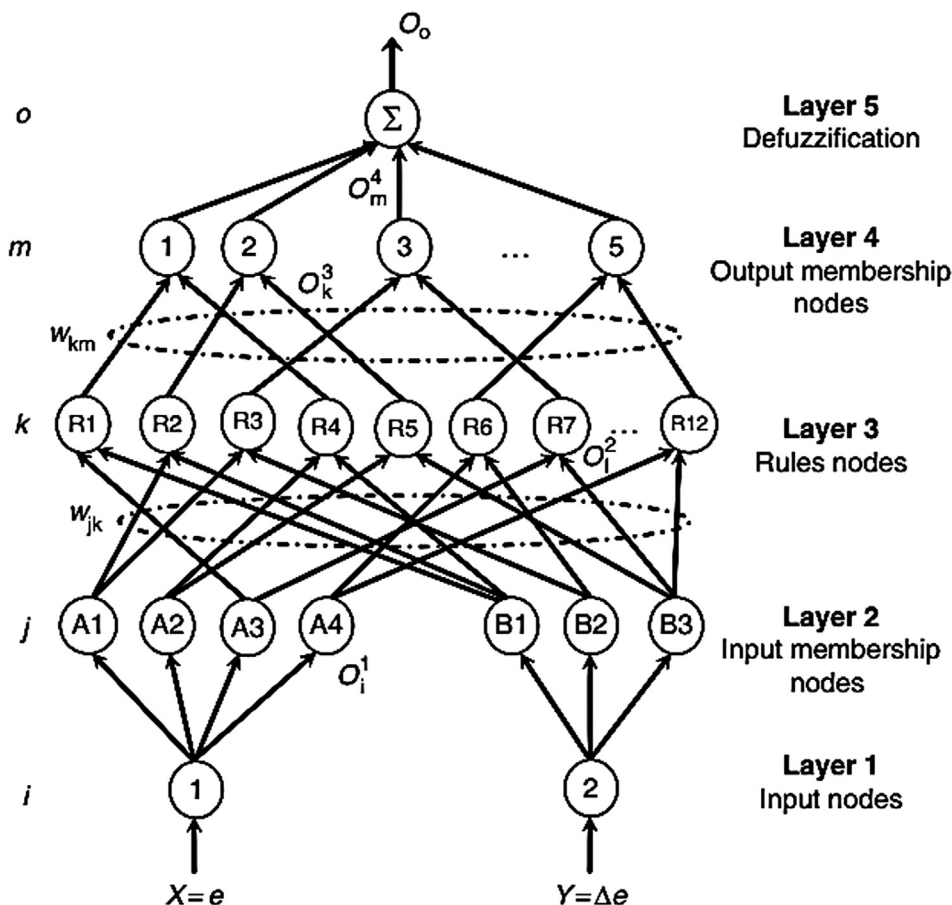


Fig. 20. ANFIS network architecture [78].

4.2.3. Optimized intelligent controller

Intelligent controllers dominate over the conventional controller in terms of prediction and control of any complex system. However, the superiority of intelligent controllers depends on the selection of controller parameters. For instance, the performance of the ANN controller is influenced by hidden layer neurons, the activation function, and the training algorithm. In addition, the capability and efficiency of FLC rely on the type of MFs [89]. Ideal parameter selection is typically carried out by the trial-and-error method. However, the trial-and-error approach requires a significant amount of time and human labor until favorable results are obtained. Thus, various optimization techniques have been introduced to select correct parameters and achieve satisfactory solutions. Recently, heuristic optimization techniques have become prominent because of their high flexibility, robustness, and efficiency in solving complex problems. Numerous heuristic optimization methods have been introduced, and these include the genetic algorithm (GA) [90], particle swarm optimization (PSO) [91], gravitational search optimization (GSA) [92], backtracking search optimization (BSA) [93], lighting search algorithm (LSA) [94], firefly algorithm (FA) [95], bat algorithm [96], and differential search algorithm (DSA) [97].

5. Power electronics application in carbon emission reduction

5.1. Motor drives

The motor is regarded as the most energy-consuming equipment in industrial applications. An efficient motor design with an efficient controller can save a substantial amount of energy. The reduced amount of energy can decrease the associated fossil fuel burning in power plants, thereby decreasing carbon emissions. Controllable

semiconductor devices are utilized for controlling motor parameters in an induction motor (IM) [98]. In addition, microcontrollers, a digital signal processor (DSP), and a field programmable gate array (FPGA) can be integrated into the IM controller design to overcome the fundamental challenges of motor control [99,100]. Previously, the current, voltage, flux, and torque of IM were controlled using conventional controllers, such as PI, PD, and PID. However, the performance of a conventional controller in controlling IM is unsatisfactory. Therefore, numerous studies have been conducted on developing AI controllers, including ANN, ANFIS, and FLC, to improve performance and reduce emissions [101].

FLC has become popular in IM control operations. FLC does not require a mathematical model and has strong computation capability to handle linear and nonlinear systems [102]. However, the performance of FLC depends on the input and output of MFs, selection of the number of MFs, and selection and operation of the rule base. These variables are determined by a heuristic procedure, which is time consuming [103]. Fig. 21 shows FLC-based optimization for indirect field-oriented control (IFOC) of an IM drive.

In [104] V/f control with FLC is employed in the IM drive to achieve a stable power level in a DC grid. IM uses FLC in vector control [105] and direct torque control (DTC) [106]. In [107], torque and speed tracking difficulties are addressed using FLC in a doubly fed IM. In [108], the space vector pulse width modulation (SVPWM) of a three-level inverter of IM is controlled using FLC with IFOC. In [109], the stator winding fault in IM is predicted using FLC with a multi-scale entropy algorithm. In [110,111], the variable speed of a wind turbine is regulated using FLC in a dual star induction generator [110]. In [112], FLC is applied in a single-phase self-excited induction generator to obtain a steady-state operation. In [113], five-phase IM is controlled by an FLC-based IFOC. In [114], DTC based on FLC is adopted to enhance

Table 5
Comparison of controller performance.

No.	Conventional controller	ANN controller	ANFIS controller	FLC controller
1.	Easy design and simple construction	Moderately complex design and normal construction	Moderately complex design and complex construction	Easy design and simple construction
2.	Needs a mathematical model	Does not need a mathematical model	Does not need a mathematical model	Does not need a mathematical model
3.	Does not require a large amount of data and learning step	Requires learning step and a large amount of data for appropriate training	Requires a learning step and large data for training	Does not require a learning step
4.	Satisfactory performance depends on the best values of PID parameters	Satisfactory performance depends on the selection of activation function, nodes, and data training	Satisfactory performance depends on the appropriate type of MFs and data training	Satisfactory performance depends on the best boundaries for input and output MFs

the dynamic control of IM drives. In [115], FLC is also employed in a permanent magnet synchronous motor (PMSM) to improve performance efficiency and save a significant amount of energy. In [116], FLC is used in a DC motor to enhance operation, efficiency, and energy conservation. In [117], FLC-based IFOC is applied to increase the efficiency improvement in three-phase IM. In [118], the inverter of three-phase IM is controlled by FLC. In [119], FLC operates the inverter turn-off angle of IM to achieve an optimum torque output. In [120], a comparative analysis of conventional PI and FLC is performed for IFOC of an IM drive.

5.2. Electric vehicles

Diesel- and gasoline-based vehicles account for 24% of global emissions [19]. Hence, electric vehicles (EVs) are regarded as a promising alternative to diesel-based vehicles due to their potential to address global warming effects. The efficiency of EVs depends on energy storage performance. However, various issues arise in relation to energy storage devices, and these include charge estimation, charge equalization, power management, temperature control, fault diagnosis, and protection. Each of these issues can be addressed by developing appropriate power converters and efficient controllers [121].

Among the various issues mentioned above, battery charge equalization in EVs has become a popular research topic in recent years. A large number of energy storage devices employed in EVs are influenced by charge imbalance due to the variation in their physical properties after several charge–discharge cycles [122]. Consequently, battery overcharging and over discharge occur, which reduce the battery’s lifespan [123]. Numerous studies have been conducted on charge equalization techniques, which are categorized into two groups, namely, passive and active [124]. Passive charge controller (PCC) includes a resistor or analog shunting and has an easy design and execution. However, PCC entails a high heat loss [125]. Active charge controller (ACC) uses inductors, capacitors, transformers, and converters to transfer or carry energy from an overcharged cell or to an overdischarged cell [126]. Inductor- and transformer-based ACCs require short duration for equalization but entail a magnetizing loss [127]. Capacitor-based ACC has a simple construction but suffers from long equalization time and ripple current [128]. Buck–boost [129], flyback [130], and resonant [131] are efficient controllers in EV operation due to their high efficiency, quick response, low stress, and bidirectional capabilities; however, they have negative points, such as high price, energy loss, and complex structure.

In [132], an intelligent charge equalization controller (CEC) was developed to achieve fast equalization and good efficiency in electric vehicle (EV) applications. The proposed CEC model includes series-connected lithium-ion battery cells connected in series, a flyback converter, cell switches, a DC–DC converter, and an equalization algorithm controlled by a microcontroller, as presented in Fig. 22.

In [134], low-voltage-stress, modularized charge equalization for a lithium-ion battery was proposed. In [135], multiple transformer-based modularized battery equalizer was suggested to reduce the equalization time. FLC was introduced to regulate the equalization current and duration. In [136], a bidirectional Cuk converter-based FLC was proposed to control the charging and discharging of series-connected lithium-ion batteries. In [137], cell balancing was carried out using state of charge (SOC) with an energy sharing concept. In [126], a battery monitoring integrated circuit (IC)-based modularized charge equalizer model was established. A prototype was designed using 88 lithium-ion batteries. In [138], a bidirectional flyback converter-based cell equalizer featuring high energy efficiency was proposed. The model was validated by designing a prototype with 12-cell series connected lithium iron cells, which exhibited high efficiency and quick cell-balancing process.

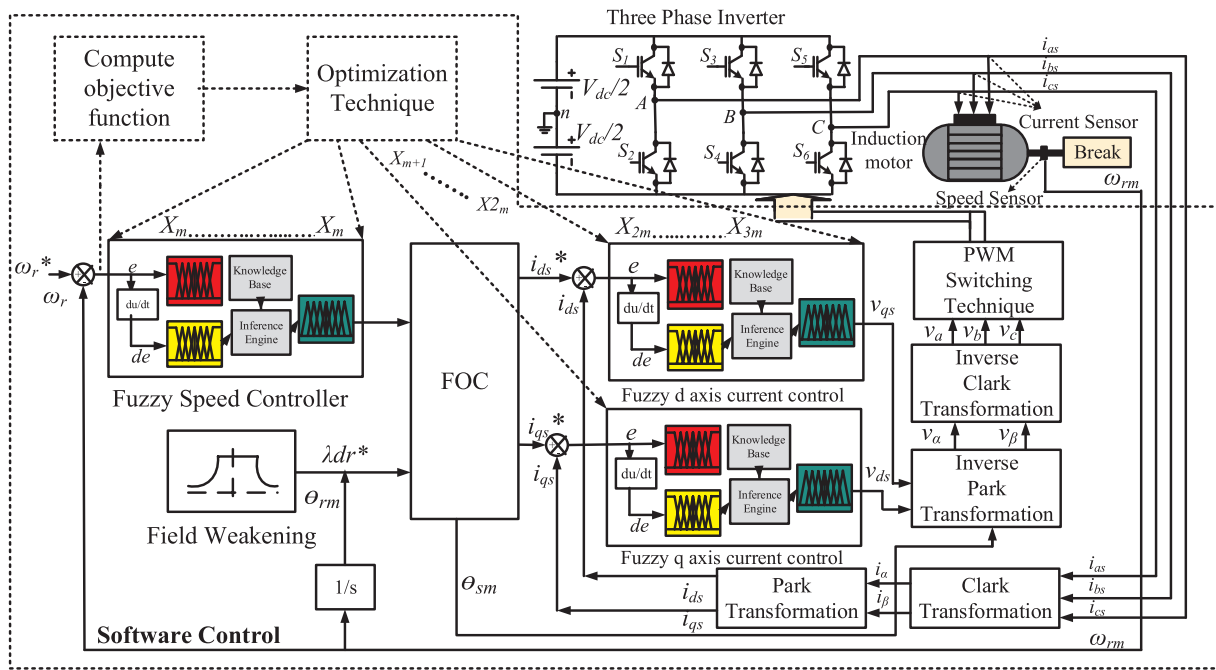


Fig. 21. FLC controller with optimization technique for IFOC [83].

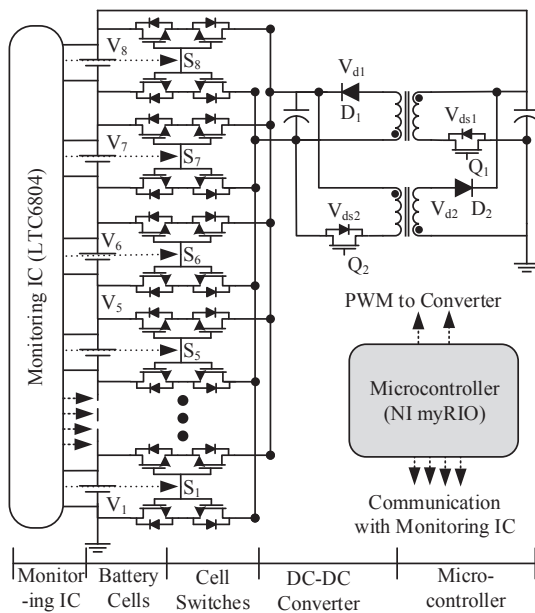


Fig. 22. CEC for lithium-ion battery pack in EV operation [133].

5.3. Renewable power generation

This section demonstrates the effectiveness of renewable electricity generation enabled by various converters and controllers. Solar PV and wind energy systems are highlighted.

5.3.1. Solar PV system

Solar PV system is a popular RE source that can deliver clean, green, reliable, and infinite power supply. A solar PV operates either as a standalone mode or grid-connected mode [139]. However, the low conversion efficiency of solar panels and intermittent solar irradiation prevent the provision of satisfactory outcomes. Therefore, a suitable power electronic circuit is required for power conversion and extraction of the maximum irradiation from sunlight [140].

For a grid-integrated solar PV system, a high-efficiency DC-AC converter is employed to convert DC power generated by a solar PV generator to AC power [141]. Nevertheless, the development of grid-connected solar PV is a challenge due to the low output voltage characteristics of solar PV. To address the challenge, high-efficiency DC-DC converters that can provide a step-up voltage gain for grid integration are used [142]. Generally, a three-phase inverter has low harmonics, high efficiency, and good performance; thus, it is suitable for the grid-connected solar PV system [143]. The structure of the three-phase inverter is derived from single-phase inverter topologies.

In [144], a transformerless, three-phase, three-level neutral point clamped (NPC) inverter system based on the grid-connected solar PV system was designed (Fig. 23). The entire system was constructed with a PV array, DC/DC converter, LC filter, three-level NPC inverter, and utility grid. Each of the three legs of the inverter comprises four power switches, four freewheeling diodes, and two clamping diodes. Five voltage levels, namely, V_{dc} , $+V_{dc}/2$, 0 , $-V_{dc}$, and $-V_{dc}/2$, are generated on the utility grid based on the switching frequency. The three-level stacked NPC structure has advantages of having double switching frequency and parallel load paths.

In [146], a grid-connected PV system using a buck-boost converter was reported to exhibit good performance, high efficiency, and a capacity to deliver maximum power under different environmental conditions. In [147], a novel power management approach was adopted to develop a hybrid wind-PV system using an inverter operating in on-grid and off-grid conditions. In [148], an improved power control strategy with high efficacy, stable operation, and fast dynamics and transition was proposed. In [149], a DC-DC converter with robust continuous-time model predictive control (CTMPC) was designed to regulate PV output voltage for a grid-connected PV system. In [150], a novel ANFIS-based PID controller was proposed to control the voltage of a three-phase grid-connected solar PV system under oscillation conditions. In [151], a novel modular multilevel converter-based PV system was introduced under the partial shading effect. In [152], a cost-effective sensorless grid-connected PV system was developed based on maximum power point tracking control and constant power generation (CPG) control. In [153], a single-phase PV grid-connected system was constructed with a boost chopper and a DC-AC inverter on the basis of fuzzy neural network (FNN). In [154], two series-connected solar PV

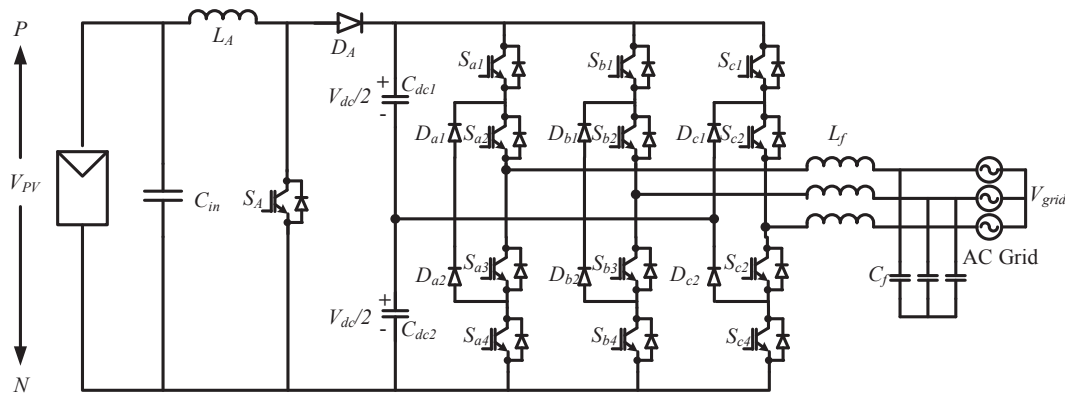


Fig. 23. Transformerless, three-phase, three-level NPC inverter system [145].

subarrays based on a grid-connected, single-phase transformerless inverter was proposed.

5.3.2. Wind energy conversion systems

Wind energy conversion systems (WECSs) have become a promising RE source due to their high efficiency, enormous capacity, and cost effectiveness. Globally, the installed capacity of WECS has increased to above 280 GW [155] and is expected to be approximately 1900 GW by 2020 [156]. The advancement of power converters and controllers helps to integrate WECS into the utility grid [5]. Nevertheless, WECSs have fluctuating wind speed, which hampers performance and efficiency [6]. Therefore, an appropriate power electronic converter (PEC) is necessary to achieve stable output power.

Numerous investigations have been carried out on wind energy converter topologies in order to achieve stable output power and improve efficiency. The various converter topologies for wind power application are illustrated in Fig. 24. The diode rectifier based converter is structured using diode rectifier and controlled inverter. This converter has an easy implementation, low production cost but suffers from high harmonics losses. Back to the back converter is built using two conventional pulse width modulation (PWM) based VSIs, a controlled rectifier, and DC-link voltage. This converter offers bidirectional power flow control; however, the execution is constrained by switching losses. The matrix converter is designed using filter and an array of bidirectional switches. This converter exhibits low switching loss, low thermal stress, high efficiency, and enhanced life cycle but has drawbacks including low output voltage, high conduction loss and complex execution in terms of modulation and commutation control. Z-source converter is based on inductors, capacitors connected in X shape, diode, and switches. This converter demonstrates high efficiency, low cost, small size but has disadvantages including unidirectional power control and power surges. Cycloconverter is known as frequency converter which can convert AC to AC directly without the need of intermediate DC-link. This converter features compact design, low conduction losses, and bidirectional power control; however, has weakness in input power factor. The multilevel converter is suitable for high power applications which is constructed using a series of switching devices. Neutral point clamped (NPC), a flying capacitor (FC) and series connected H-bridge (SCHB) converter topologies are used in common as multilevel converters. This converter has strong points in terms of reduced size, low switching loss, high efficiency, high voltage handle capability but has limitations including complex circuit design, voltage imbalance and unequal current stress [157].

In [158], ANN based wind energy systems are reviewed in terms of forecasting, predictions, design and control optimization, fault detection and diagnosis. In [159], the design and control of DFIG-based grid connected WECS were analyzed. In [160], a hybrid ANFIS-GA-based WECS was proposed to improve performance. In [161], matrix converter-interfaced DFIG-based WECS was investigated at various wind

speeds. In [162], a novel fractional order-sliding mode control (FOSMC)-based WECS of DFIG was proposed to control active and reactive power. In [163], partial feedback linearization (PFL) controller-based series-compensated DFIG was proposed to reduce the sub-synchronous control interaction (SSCI). In [164], a dynamic model of DFIG was developed to regulate DC-link voltage control. In [165], an impedance model of DFIG was constructed to control multiple high frequencies. In [166], a robust state feedback control-based DFIG was constructed using perturbation estimation for maximum power extraction of DFIG. In [167], a grid-connected DFIG was presented to evaluate the dynamic performance and control damping oscillation. In [168], a novel DC grid-interfaced DFIG-based WECS was developed.

5.4. Power quality enhancement

RE penetration and increasing amount of nonlinear load have been identified as having an extensive influence on power quality (PQ) issues [169,170]. PQ disturbances occur due to current and voltage oscillation injected from nonlinear load. PQ problems result in serious impacts on the power system network, such as high harmonics, load unbalancing, overheating, low power factor, sag, and flicker [171,172]. PQ disturbances cause a huge power loss in the transmission and distribution networks, which subsequently increase the power consumption and global emission. Therefore, an investigation is required on PQ mitigation methods to enhance the quality of power supplied.

5.4.1. Flexible alternating current transmission system (FACTS)

FACTS has been successful in addressing PQ disturbances. FACTS is made from power electronic devices. FACTS devices are classified into four groups [173] such as series FACTS devices, shunt FACTS devices, combined series-series FACTS devices and combined shunt-series FACTS devices, respectively. Series FACTS devices include a thyristor-controlled series capacitor (TCSC), thyristor-controlled phase-shifting transformer (TCPST), and static synchronous series compensator (SSSC). Shunt FACTS devices contain static VAR compensator (SVC) and static synchronous compensator (STATCOM). Combined series-series FACTS devices comprise interline power flow controller (IPFC) and combined shunt-series FACTS devices, such as unified power flow controller (UPFC) [174,175].

5.4.2. Distribution static compensator (DSTATCOM)

STATCOM has been applied successfully in power distribution systems due to its attractive features, such as flexible controllability, fast response, small size, low power loss, superior performance in limiting harmonics, and transient voltage. A distribution static compensator (DSTATCOM) consists of a voltage source inverter and current controlled insulated gate bipolar transistors (IGBTs). Fig. 25(a), (b), (c), and (d) illustrate the various topologies and control techniques of DSTATCOM for PQ improvement using star-delta, T-connected, zig-zag,

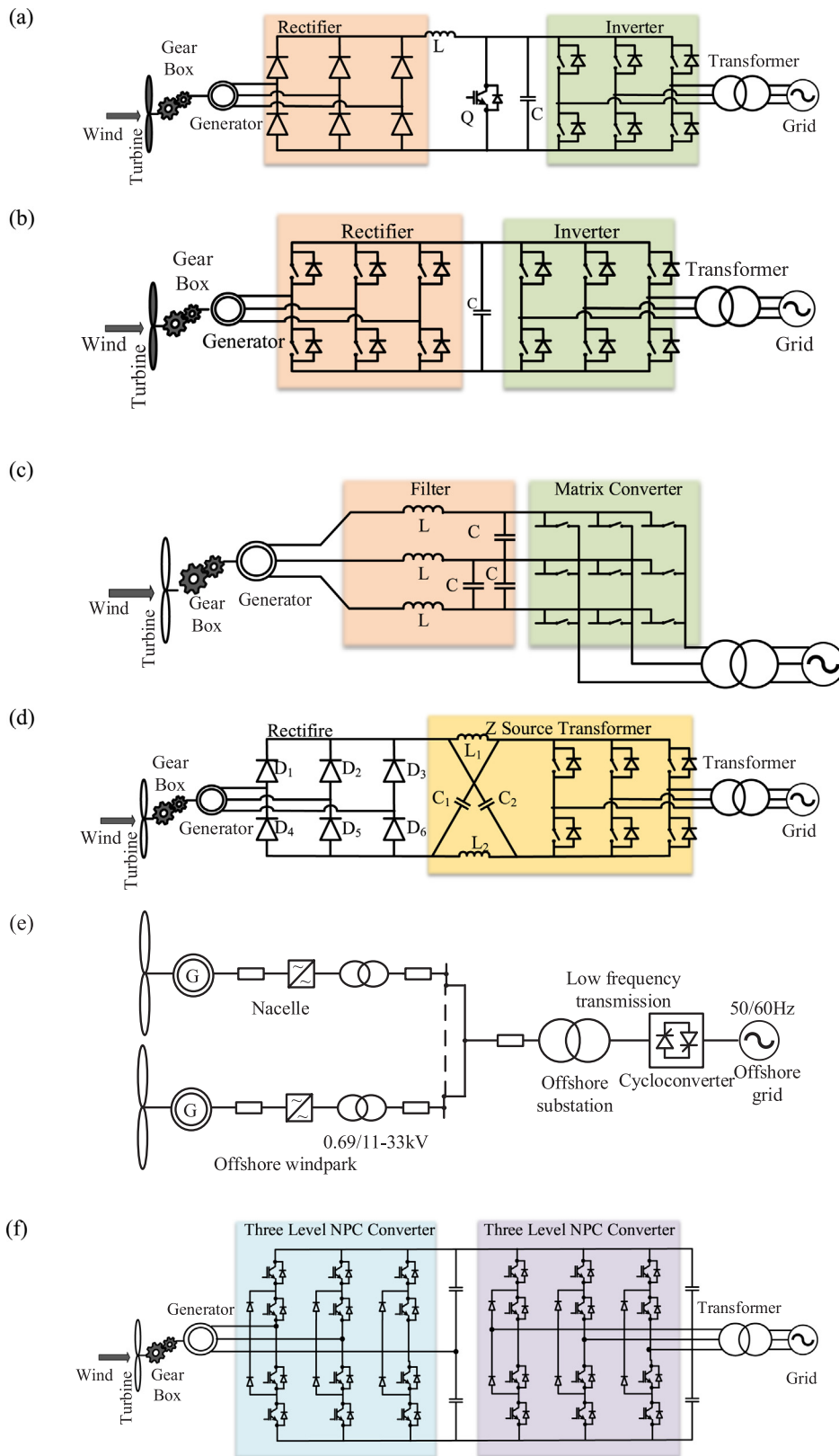


Fig. 24. Wind energy converter topologies (a) diode rectifier based converter, (b) back to back converter, (c) matrix converter, (d) Z-source converter, (e) Cycloconverter (f) Multilevel converters [157].

and star-hexagon transformer, respectively [176]. Numerous studies have been conducted on the control techniques of DSTATCOM for PQ enhancement. Immune algorithm- [163] and firefly algorithm [163]-based DSTATCOM is utilized to determine the optimal location in the

distribution system. In [164], the fuzzy multi-objective approach and ant colony optimization were employed to search for the optimal size and location of solar PV and DSTATCOM. In [165], DSTATCOM-based WECS was developed to evaluate the thermal stress and reliability of a

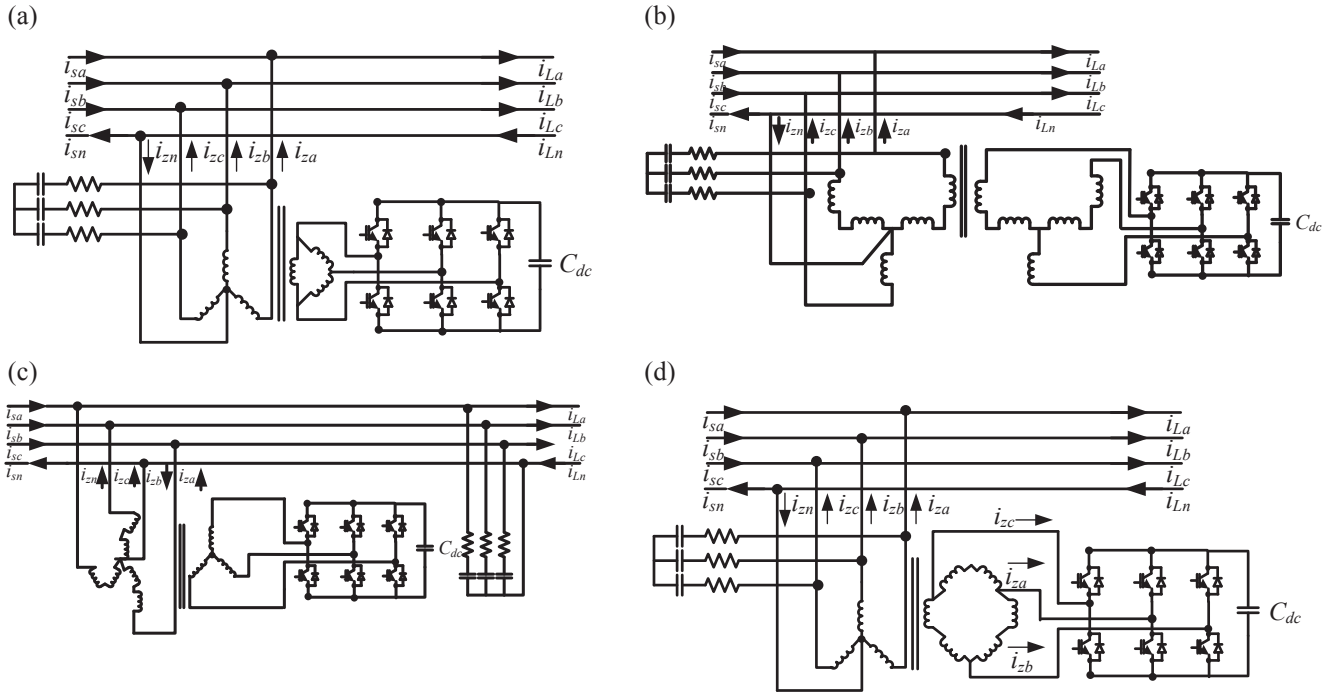


Fig. 25. Three-phase four-wire DSTATCOM topology using (a) star-delta, (b) T-connected, (c) zig-zag, and (d) star-hexagon transformer [176].

microgrid. The use of DSTATCOM has also been reported in reactive power compensation [166], voltage regulation [167], power quality enhancement [168], low voltage distribution [169], and load compensation [170].

5.5. Efficient electricity transmission

RE in the form of wind energy has more power generation in offshore than onshore owing to the better wind velocity in offshore areas. Nevertheless, high voltage alternative current (HVAC) is inappropriate for offshore wind resources due to the high transmission cost and power loss [177]. When consumers are located extremely far from the wind resources, the power grid becomes unstable and creates various troubles, such as oscillation, harmonic distortion, voltage drop, and frequency deviation [178]. Therefore, high voltage direct current (HVDC) has become an attractive alternative for long-distance power transfer. HVDC transmission systems are designed using either a voltage source converter (VSC) [179] or a current source converter (CSC) [180]. VSC HVDC has excellent controllability, reliability, and flexibility; thus, it is frequently used in short and long transmission systems [181].

5.5.1. VSC-based HVDC

Various VSC based HVDC topologies have been reported in literature such as a two-level converter, three-level converter, modular multilevel converter (MMC) and hybrid VSC [182,183]. The two-level converter is designed using series-connected IGBTs with inverse parallel diodes and DC capacitors as shown in Fig. 26(a) [184]. This type of converter exhibits high switching loss, low efficiency but suffers from electromagnetic interference (EMI) problem. The three-level converter is configured using DC capacitor, diode valve, and IGBT switches, as presented in Fig. 26(b) [185]. This topology has improved the harmonic performance of the converter by employing three discrete voltage levels $+\frac{1}{2} U_d$, 0 and $-\frac{1}{2} U_d$ of the AC signal. The modular multi-level converter (MMC) is structured using six valves installed in three submodules (SM), as shown in Fig. 26(c) [186]. Each valve in MMC is configured with a controllable voltage source and storage capacitor. The hybrid VSC is a combination of two-level and MMC converters which is designed using H-bridge converters, M2C cells as shown in

Fig. 26(d). H-bridge converters comprise series IGBTs to provide the desired voltage at the fundamental frequency [187].

VSC-based HVDC transmission systems use vector control to regulate active and reactive power independently. However, instability in VSC-HVDC has been reported due to the phase lock loop (PLL) while integrating with a weak AC grid. Hence, improved vector control with four decoupling gains is employed for the proper coordination of VSC-HVDC and weak AC grid (ref). Fig. 27 shows VSC-HVDC with power synchronization control (PSC). PSC synchronization is based on the power angle relationship. PSC is executed by regulating the active power of the converter and evaluating the output power angle for the VSC PWM unit. The mathematical expression of PSC is shown as

$$\theta(s) = \frac{K_p}{s}(P^*(s) - P(s)) \quad (22)$$

$$\omega t_{PSC} = w^*t - \Delta\theta, \quad (23)$$

where $\frac{K_p}{s}$ is the integral controller, θ is the synchronization angle, and ω denotes frequency.

In a fault condition, proper synchronization between the converter and grid is performed using a backup PLL-based current limitation algorithm. Reactive power control with inner loop voltage control is designed to control the converter reactive power.

VSC-HVDC has been implemented in transmission systems to address various problems. In [192], a novel electromagnetic theory- and circuit theory-based VSC-HVDC was introduced to investigate the radiated electromagnetic disturbance (EMD). In [193] Newton-Raphson method-based VSC-HVDC was proposed to control DC voltage. In [194], a motion equation concept-based PLL-synchronized VSC HVDC was proposed to maintain the standardized frequency in an islanded system. In [195], a VSC-HVDC-based transient management system was developed to improve the fault ride-through (FRT) performance. In [196], droop control-based VSC-HVDC was presented to improve DC voltage. In [197], VSC-HVDC was applied in wind farms to analyze the transient response. In [198], VSC-HVDC was proposed to address short-circuit current. In [199], VSC-HVDC was employed for impedance matching. In addition, VSC HVDC was successfully implemented in fast frequency response [200], reactive power coordination [201], protection [202], power-sharing control [203], overvoltage control [204], small-signal

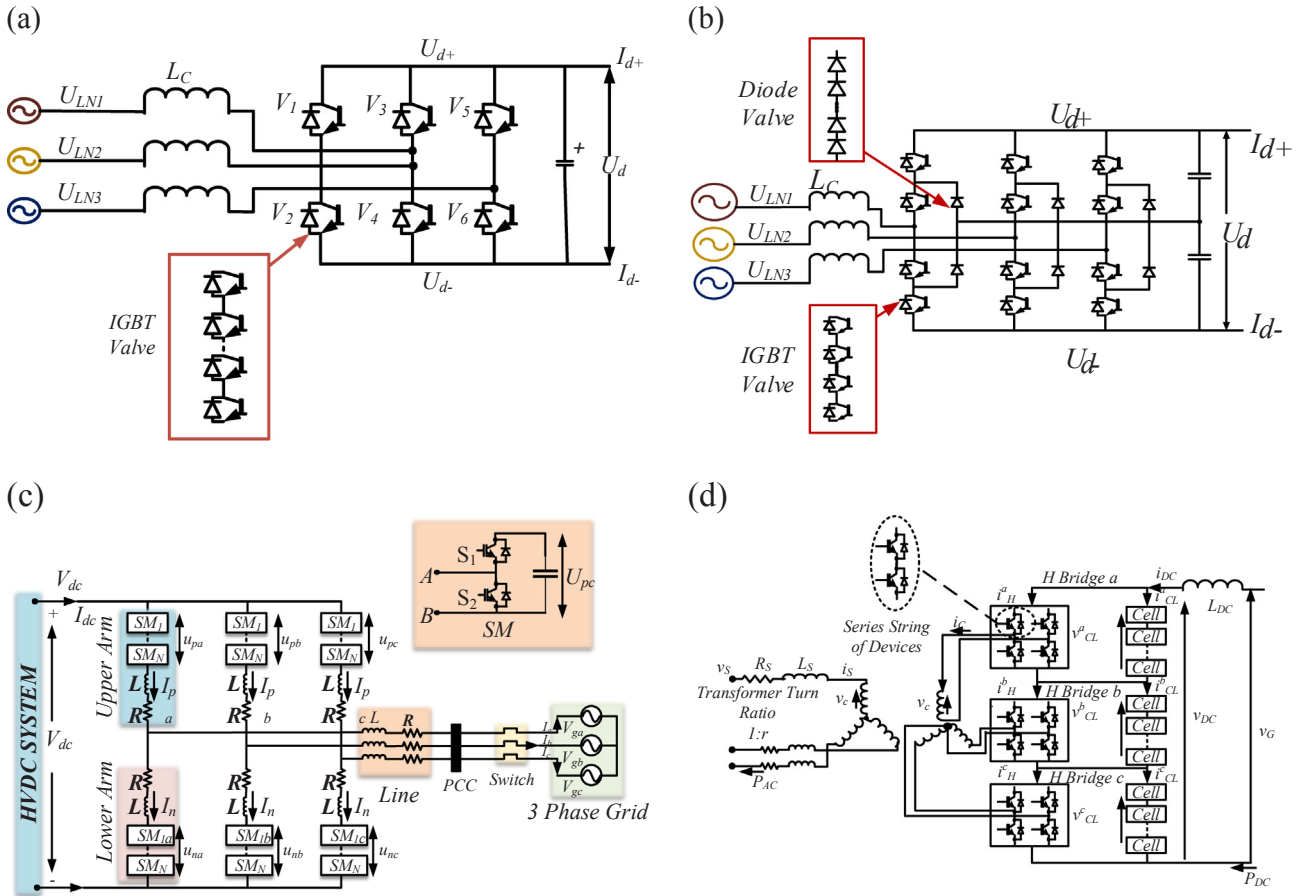


Fig. 26. Converter topology in HVDC system (a) Three-phase, two-level VSC based HVDC topology [188] (b) Three-phase, three-level, diode-clamped VSC based HVDC topology [188] and (c) Three-phase MMC topology [189] (d) Three-phase hybrid VSC topology [190].

stability analysis [205], and grid synchronization [206].

5.6. Energy storage system

The applications of energy storage technologies in smart grids and microgrids have received massive attention due to their huge contributions in reducing carbon emissions. A sustainable and economic electricity supply can be secured by adopting proper coordination between energy storage devices and loads. However, appropriate coordination depends on the switching and control of the energy storage system (ESS) interfaced with the utility grid. Therefore, a power converter or controller with characteristics of enhanced performance and rapid response are mandatory to handle dynamic conditions of smart

power grids. In a grid-connected ESS system, the power converter converts from one form to another while ensuring that reliability, efficiency, and flexibility are maintained. Then, power electronic controllers are employed to control ESS charging–discharging and thus prolonging life expectancy.

In [207], a grid-connected ESS with electrochemical batteries or supercapacitors was designed, as shown in Fig. 28. The entire system is configured using ESS, DC-DC converter, three-phase VSI, filter, and utility grid. ESS is connected to a dual buck/boost DC/DC converter to improve the performance of the entire system. The main topology of this structure is VSI, which uses IGBTs and sinusoidal pulse width modulation (SPWM) to achieve a smooth output voltage. Active and reactive power control between ESS and the utility grid is determined

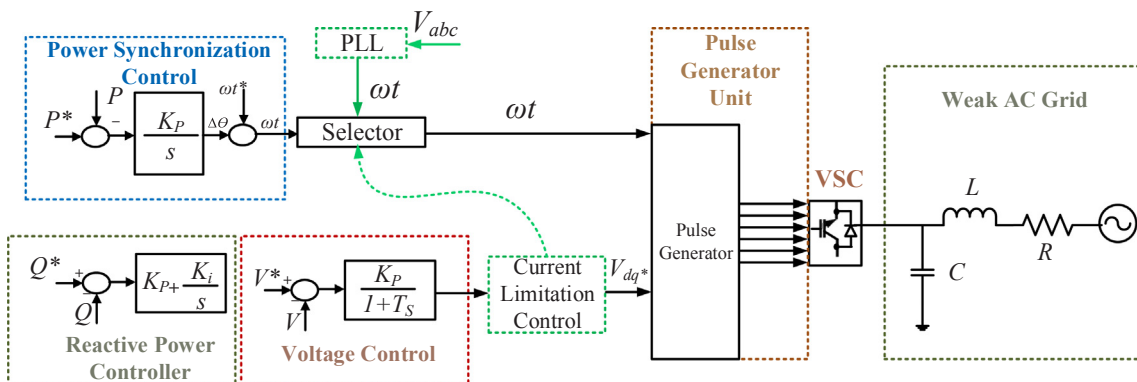


Fig. 27. AC grid improvement using VSC-HVDC with PSC [191].

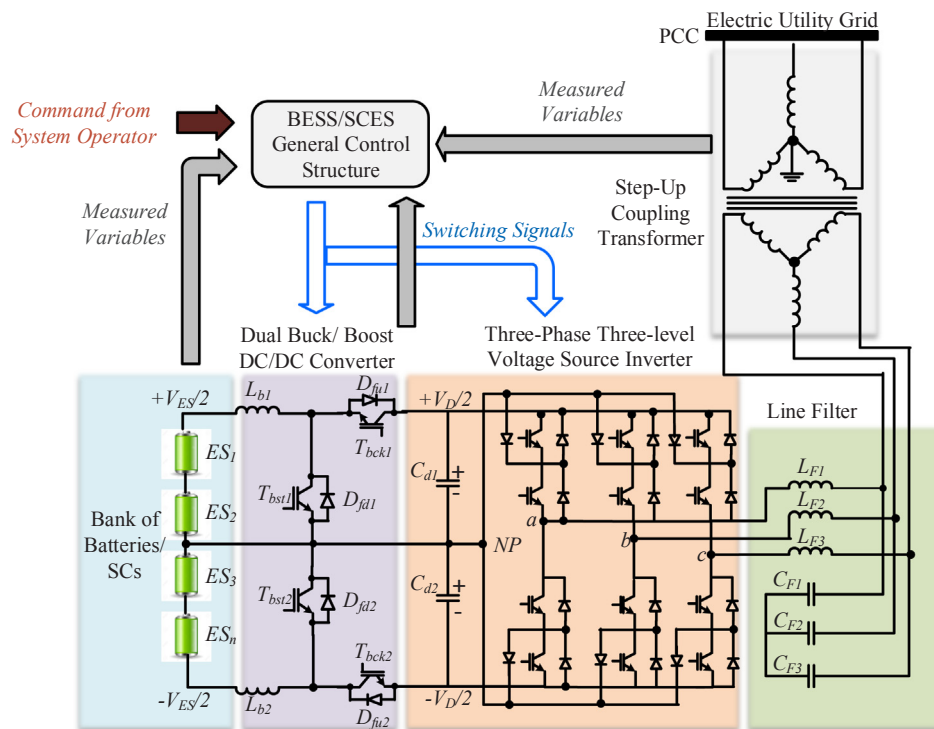


Fig. 28. Structure of grid-connected ESS [207].

by switching signals.

In [208], a grid-connected DC–AC inverter controller-based ESS was proposed for stability enhancement. In [209], optimal controller-based flywheel ESS was developed to stabilize the output of DFIG. In [210], grid-connected hybrid RE generation-based ESS was presented to control active and reactive power. In [211], grid-connected AC/DC converter-based ESS was introduced to optimize transient operations. In [212], the multi-temporal deterministic approach-based grid-connected energy storage management system was proposed. In [213], a residential grid-connected ESS was developed on the basis of FLC. In [214], a detailed comparison of grid-connected ESS was performed. Furthermore, grid-connected ESS was designed to study economic dispatch [215], phase balancing [216], demand response [217], sizing [218], and scheduling [214].

6. Energy conversion issues and potential recommendations

The International Energy Agency (IEA) has identified that RE integration and reduction of fossil fuel dependency could be major tools in combating global warming. The principles of harnessing RE into grids or daily usage require a power electronic converter and its controller. Despite its perceived simplicity, harnessing or converting reliable or sustainable energy from one stage to another is actually challenging. Accordingly, this section highlights the issues, challenges, potential recommendations of energy converters and their controller and applications.

6.1. Issues and challenges

6.1.1. Power electronic converter

Power converters have a few disadvantages because they inject harmonics on both the supply and load sides. On the supply side, harmonics cause overheating and efficiency reduction in the transformer. In addition, harmonics result in a frequency interference problem, which may damage the equipment. Harmonics may also provide a skin effect, which increases the likelihood of overheating. On the load side, harmonics provide excessive heating. Apart from these, reactive power

compensation equipment must be installed for low-power-factor power electronic converters. In summary, appropriate filter and safety arrangement are compulsory for converter protection and operation.

6.1.2. Power electronic controller

The performance of the conventional controller is unsatisfactory due to its vulnerability to temperature variation and load disturbances. By contrast, activation function, training algorithm, MFs, and hidden layer neurons are selected based on the trial and error approach in conventional FLC, ANFIS, and ANN structures. Nevertheless, the trial and error approach is a highly ineffective approach and consumes a significant amount of time and human energy. Thus, an intelligent controller is configured with optimization technique to improve the performance efficiency of the converter, which in turn reduces emission and global warming.

6.1.3. Renewable energy converter

Implementing RE to an electricity grid is a complex task and must include the appropriate converter and controller for proper synchronization [219]. Solar PV and WECS suffer from voltage instability, poor power quality, low efficiency, grid congestion, operational restriction, and protection. Therefore, investigations must be performed on converter and controller design to reduce oscillation while improving performance and reliability.

6.1.4. Electric vehicle battery

Converter-based CEC faces problems of voltage and current stresses on MOSFET switching drives. The stresses may harm the switches during equalization because discontinuity occurs while balancing the battery stack. Thus, an efficient CEC model must be developed with a simple design, implementation, and improved equalization performance for EVs. In addition, the battery is highly sensitive to aging, temperature variation, and charge–discharge cycles [220]. A substantial effect occurs on battery capacity when the temperature of the battery decreases or increases beyond the threshold limit [221]. Aging can cause degradation in resistance and capacitance, which eventually reduces the energy density and lifespan of the battery [222]. Battery

safety and protection have a significant impact on system operation and market acceptance. Therefore, a battery management system (BMS) with sufficient safe circuitry is required to ensure a secure operation of EVs, which in turn reduces carbon emissions.

6.1.5. RE converter implementation

A major concern for the proper control functioning of the control system is the hardware design and implementation of power electronic converters. The most extensively used integrated circuits for controller design are dSPACE [223], field programmable gate array (FPGA) [224], and digital signal processor (DSP) [100]. However, dSPACE and FPGA have the disadvantage of high cost and operational constraint in standalone mode. DSP outperforms dSPACE and FPGA owing to its low power consumption, fast response, and operational capabilities in standalone mode. Nonetheless, the design and execution of DSP require extensive research and rigorous knowledge on operating and controlling an embedded system. In many developing countries, high borrowing cost is already creating an obstacle for RE sector growth. Although project financing is available for the majority of RE power projects with a 70:30 debt equity ratio, the high interest rates under difficult macroeconomic conditions create problems in implementing this technology.

6.1.6. Grid-connected RES power quality issues

Despite the presence of a stable grid, integrating RES into the grid leads to potential technical issues owing to the intermittent nature of RES and thus affects the PQ problems. During energy conversion, the main parameters affecting the major PQ problems include voltage fluctuations, power system transients and harmonics, reactive power, low power factor, electromagnetic interference, and synchronization. Moreover, the availability of renewable energy is variable owing to the weather pattern, solar radiations, cloud day & night cycles, storms/turbulence, and so on. Moreover, variations in voltage and grid frequency create difficulties in RE operations and reduce the chances for successful RE integration into the grid. Nonetheless, the problem of grid integration can also be solved by using power electronic concepts. Thus, to confront future RES power grid integration, robust design and optimal operation of the power electronic converter systems are highly important in minimizing the PQ issues.

6.2. Potential recommendations

This review has proposed a few potential and selective recommendations for the further technological development of power electronic technology in reducing global warming, such as the following:

- Further study should be conducted on the power electronic converter design to improve capacity, power factor and remove harmonics switching stress.
- The development of an intelligent and robust controller in solar PV, WECS, and ESS requires further attention.
- Various optimization techniques, such as LSA, BSA, PSO, and FA, can be employed to determine the optimal values and minimum error of ANN, ANFIS, and FLC.
- Further research should be performed on the hardware implementation of the power electronic controller using dSPACE, FPGA, and DSP.
- An improved technology during ESS manufacture and disposal is required to reduce the negative environmental impacts and health issues. Further attention is also needed to develop the machinery for recycling to enrich the reservation of ESS and to reduce the CO₂ and GHG emissions.

These recommendations would be a significant contribution toward the development and implementation of power electronic converters

and controllers and would provide a concrete idea for researchers and manufacturers about the advancement of power electronic contributions toward carbon emission and global warming reduction.

7. Conclusion

An extensive review of various power electronic technologies for mitigating global warming is carried out. The review outlines a detailed investigation of power electronic converters, controller topologies, and associated implementation in different applications to identify their substantial contribution to saving energy and mitigating the global warming effect. The review starts with an explanation of the global warming potential, related causes, and impacts on the environment. The power converter structure, operation, strengths, and weaknesses are then analyzed. Subsequently, the classification of controllers, including conventional and intelligent, with their algorithms, mathematical models, benefits, and drawbacks is presented. Finally, the review provides the execution of the power converter and controller in different applications, including motor drives, electric vehicles, solar PV, wind energy, FACTS, HVDC, and energy storage. It then highlights how energy saving and carbon emission reduction take place. An AC–DC converter has low conduction and switching loss but suffers from low power factor and high harmonic distortion. A DC–AC converter has low stress and harmonics but exhibits high conversion loss. A DC–DC converter demonstrates fast response and high efficiency but shows weakness in terms of high switching loss. An AC–AC converter achieves high efficiency but has drawbacks with regard to large size and high harmonics. Conventional controllers have a simple design, require mathematical equations, and do not need a learning step. By contrast, intelligent controllers have a complex structure, do not require a mathematical model, and need a learning step and big data to train. Moreover, intelligent controllers obtain good performance when a suitable training algorithm, number of nodes, and type of MFs are selected. The main contribution of this review is that it highlights power electronic technologies, existing issues and challenges, and their contributions, applications, and recommendations in mitigating carbon emission and global warming.

Acknowledgement

This work is supported by the Ministry of Higher Education, Malaysia Grant no. 20190101LRGS under the Universiti Tenaga Nasional.

References

- [1] Narbel PA, Hansen JP. Estimating the cost of future global energy supply. *Renew Sustain Energy Rev* 2014;34:91–7.
- [2] Global Energy Institute. <https://www.globalenergyinstitute.org/international-energy-agency-releases-its-world-energy-outlook> [accessed 22.08.18].
- [3] Silva Herran D, Tachiiri K, Matsumoto K. Global energy system transformations in mitigation scenarios considering climate uncertainties. *Appl Energy* 2019;243:119–31.
- [4] Ye B, Jiang J, Li C, Miao L, Tang J. Quantification and driving force analysis of provincial-level carbon emissions in China. *Appl Energy* 2017;198:223–38.
- [5] Lee ZH, Sethupathi S, Lee KT, Bhatia S, Mohamed AR. An overview on global warming in Southeast Asia: CO₂ emission status, efforts done, and barriers. *Renew Sustain Energy Rev* 2013;28:71–81.
- [6] Pelletier C, Rogaume Y, Dieckhoff L, Bardeau G, Pons M-N, Dufour A. Effect of combustion technology and biogenic CO₂ impact factor on global warming potential of wood-to-heat chains. *Appl Energy* 2019;235:1381–8.
- [7] Climate Change: Atmospheric Carbon Dioxide. <https://www.climate.gov/news-features/understanding-climate/climate-change-atmospheric-carbon-dioxide> [accessed 10.08.18].
- [8] Each Country's Share of CO₂ Emissions. <https://www.ucsusa.org/global-warming/science-and-impacts/science/each-countrys-share-of-co2.html#.W2aZFdzM8> [accessed 05.08.18].
- [9] Hannah Ritchie, Roser M. CO₂ and other Greenhouse Gas Emissions. <https://ourworldindata.org/co2-and-other-greenhouse> [accessed 15.08.18].
- [10] Craig CA, Feng S. Exploring utility organization electricity generation, residential

- electricity consumption, and energy efficiency: A climatic approach. *Appl Energy* 2017;185:779–90.
- [11] Zeng Z, Hong M, Li J, Man Y, Liu H, Li Z, et al. Integrating process optimization with energy-efficiency scheduling to save energy for paper mills. *Appl Energy* 2018;225:542–58.
- [12] Sperberg R, Kniss R, Ruegg T. Energy efficiency in California cement plants: energy savings potential realized by accessing utility energy-efficiency program resources. *IEEE Ind Appl Mag* 2018;24:12–6.
- [13] Bose BK. Global energy scenario and impact of power electronics in 21st century. *IEEE Trans Ind Electron* 2013;60:2638–51.
- [14] Kusumadewi TV, Winyuchakrit P, Limmeechokchai B. Long-term CO₂ emission reduction from renewable energy in power sector: the case of Thailand in 2050. *Energy Procedia* 2017;138:961–6.
- [15] Xu SC, He ZX, Long RY. Factors that influence carbon emissions due to energy consumption in China: Decomposition analysis using LMDI. *Appl Energy* 2014;127:182–93.
- [16] United States Environmental Protection Agency. Understanding Global Warming Potentials. <https://www.epa.gov/ghgemissions/understanding-global-warming-potentials> [accessed 12.08.18].
- [17] IPCC - Intergovernmental Panel on Climate Change. Climate Change Synthesis Report; 2014.
- [18] United States Environmental Protection Agency. Overview of Greenhouse Gases, Carbon Dioxide Emissions. <https://www.epa.gov/ghgemissions/overview-greenhouse-gases> [accessed 18.08.18].
- [19] IEA. CO₂ emission from fuel combustion Overview; 2017.
- [20] EU actions. Fluorinated greenhouse gases. https://ec.europa.eu/clima/policies/f-gas_en [accessed 28.07.18].
- [21] Hanaoka T, Ishitani H, Matsushashi R, Yoshida Y. Recovery of fluorocarbons in Japan as a measure for abating global warming. *Appl Energy* 2002;72:705–21.
- [22] United Nations Framework Convention on Climate Change (UNFCCC). Emissions and supply of fluorinated greenhouse gases. 2015. <https://www.eea.europa.eu/data-and-maps/indicators/emissions-and-consumption-of-fluorinated-2/assessment> [accessed 09.07.18].
- [23] Temperatures, Climate Action Tracker. <https://climateactiontracker.org/global/temperatures/> [accessed 20.08.18].
- [24] Bose BK. and Impact of Power Electronics in the Present Century; 2014.
- [25] Lu S-M. A review of high-efficiency motors: Specification, policy, and technology. *Renew Sustain Energy Rev* 2016;59:1–12.
- [26] Hossain MZ, Rahim NA, Selvaraj JA. Recent progress and development on power DC-DC converter topology, control, design and applications: A review. *Renew Sustain Energy Rev* 2018;81:205–30.
- [27] Zhang N, Sutanto D, Muttaqi KM. A review of topologies of three-port DC-DC converters for the integration of renewable energy and energy storage system. *Renew Sustain Energy Rev* 2016;56:388–401.
- [28] Zhang G, Li Z, Zhang B, Halang WA. Power electronics converters: Past, present and future. *Renew Sustain Energy Rev* 2018;81:2028–44.
- [29] Wu H, Wong S-C, Tse CK, Chen Q. Control and modulation of bidirectional single-phase AC-DC three-phase-leg SPWM converters with active power decoupling and minimal storage capacitance. *IEEE Trans Power Electron* 2016;31:4226–40.
- [30] Kolar JW, Friedli T. The essence of three-phase PFC rectifier systems—Part I. *IEEE Trans Power Electron* 2013;28:176–98.
- [31] IEEE Std. IEEE Recommended Practice and Requirements for Harmonic Control in Electric Power Systems. IEEE Std 519-2014 (Revision IEEE Std 519-1992); 2014, p. 1–29.
- [32] Alam M, Eberle W, Gautam DS, Botting C, Dohmeier N, Musavi F. A hybrid resonant pulse-width modulation bridgeless AC-DC power factor correction converter. *IEEE Trans Ind Appl* 2017;53:1406–15.
- [33] Siwakoti YP, Forouzeh M, Ha Pham N. Control of power electronic converters and systems, Chapter 1: Power Electronics Converters—An Overview. Elsevier Inc.; 2018.
- [34] Niewiara LJ, Tarczewski T, Grzesiak LM. Application of DC/DC/AC dual voltage source inverter for current harmonics reduction in PMSM drive. In: 2017 19th Eur. Conf. Power Electron. Appl. (EPE'17 ECCE Eur., IEEE; 2017, p. P.1-P.9.
- [35] Yamanaka K, Hara H, Kume T, Ishii S. Bidirectional DC-AC current source inverter using coupled inductor. In: 2012 IEEE 13th Work. Control Model. Power Electron., IEEE; 2012, p. 1–6.
- [36] Rodriguez J, Bernet S, Wu B, Pontt JO, Kouro S. Multilevel voltage-source-converter topologies for industrial medium-voltage drives. *IEEE Trans Ind Electron* 2007;54:2930–45.
- [37] Kouro S, Malinowski M, Gopakumar K, Pou J, Franquelon LG, Bin Wu, et al. Recent advances and industrial applications of multilevel converters. *IEEE Trans Ind Electron* 2010;57:2553–80.
- [38] Marzoughi A, Burgos R, Boroyevich D, Xue Y. Design and comparison of cascaded H-bridge, modular multilevel converter, and 5-L active neutral point clamped topologies for motor drive applications. *IEEE Trans Ind Appl* 2018;54:1404–13.
- [39] Shen Jie, Schröder S, Rösner R, El-Barbary S. A comprehensive study of neutral-point self-balancing effect in neutral-point-clamped three-level inverters. *IEEE Trans Power Electron* 2011;26:3084–95.
- [40] Melin PE, Rohten JA, Espinoza JR, Baier CR, Espinosa EE, Munoz JA, et al. Analysis and design of a multicell topology based on three-phase/single-phase current-source cells. *IEEE Trans Power Electron* 2016;31:6122–33.
- [41] Khoshkbar SA, Corzine K, Dargahi V. Enhanced double flying capacitor multicell power converter controlled with a new switching pattern. *IET Power Electron* 2015;8:2386–95.
- [42] Asadi F, Eguchi K, Hudgins J. Dynamics and control of DC-DC converters. *Synth Lect Power Electron* 2018;6:1–241.
- [43] Spiliotis K, Gonçalves JE, Van De Sande W, Ravyts S, Daenen M, Saelens D, et al. Modeling and validation of a DC/DC power converter for building energy simulations: Application to BIPV systems. *Appl Energy* 2019;240:646–65.
- [44] Forouzeh M, Siwakoti YP, Gorji SA, Blaabjerg F, Lehman B. Step-Up DC-DC converters: a comprehensive review of voltage-boosting techniques, topologies, and applications. *IEEE Trans Power Electron* 2017;32:9143–78.
- [45] Singh SN. Selection of non-isolated DC-DC converters for solar photovoltaic system. *Renew Sustain Energy Rev* 2017;76:1230–47.
- [46] Wang J-M, Tzeng L, Hsu M-T, Jian H-R. A simple control scheme to avoid the sensing noise for the DC-DC buck converter with synchronous rectifier. *IEEE Trans Ind Electron* 2018;65:5086–91.
- [47] Veerachary M. Analysis of minimum-phase fourth-order buck DC-DC converter. *IEEE Trans Ind Electron* 2016;63:144–54.
- [48] Wu H, Mu T, Ge H, Xing Y. Full-range soft-switching-isolated buck-boost converters with integrated interleaved boost converter and phase-shifted control. *IEEE Trans Power Electron* 2016;31:987–99.
- [49] Liu H, Ji Y, Wang L, Wheeler P. A family of improved magnetically coupled impedance network boost DC-DC converters. *IEEE Trans Power Electron* 2018;33:3697–702.
- [50] Ahmed HF, Cha H, Khan AA, Kim H-G. A novel Buck-boost AC-AC converter with both inverting and noninverting operations and without commutation problem. *IEEE Trans Power Electron* 2016;31:4241–51.
- [51] Kang F, Park S-J, Cho SE, Kim J-M. Photovoltaic power interface circuit incorporated with a buck-boost converter and a full-bridge inverter. *Appl Energy* 2005;82:266–83.
- [52] Zhou Q, Liu C, Liu X, Zhang X, Xu J, Cao K. Effect of intermediate capacitance on slow-scale instability of Cuk power factor correction converter operating in discontinuous capacitor voltage mode. *IET Power Electron* 2017;10:1975–81.
- [53] Anand A, Singh B. Design and implementation of PFC Cuk converter fed SRM drive. *IET Power Electron* 2017;10:1539–49.
- [54] Zhang Z, Lin J, Zhou Y, Ren X. Analysis and decoupling design of a 30 MHz resonant SEPIC converter. *IEEE Trans Power Electron* 2016;31:4536–48.
- [55] Moradpour R, Ardi H, Tavakoli A. Design and implementation of a new SEPIC-based high step-up DC/DC converter for renewable energy applications. *IEEE Trans Ind Electron* 2018;65:1290–7.
- [56] Singh AK, Pathak MK. Single-stage ZETA-SEPIC-based multifunctional integrated converter for plug-in electric vehicles. *IET Electr Syst Transp* 2017.
- [57] Andrade AMSS, Martins MLda S. Quadratic-boost with stacked zeta converter for high voltage gain applications. *IEEE J Emerg Sel Top Power Electron* 2017;5:1787–96.
- [58] Chen H, Zheng Z, Xiao J. Determining the number of transformer shielding winding turns for suppressing common-mode noise in flyback converters. *IEEE Trans Electromagn Compat* 2018;60:1606–9.
- [59] Roggia L, Schuch L, Baggio JE, Rech C, Pinheiro JR. Integrated full-bridge-forward DC-DC converter for a residential microgrid application. *IEEE Trans Power Electron* 2013;28:1728–40.
- [60] Li S, Xiangli K, Smedley KM. A control map for a bidirectional PWM plus phase-shift-modulated push-pull DC-DC converter. *IEEE Trans Ind Electron* 2017;64:8514–24.
- [61] Han J-K, Kim J-W, Moon G-W. A high-efficiency asymmetrical half-bridge converter with integrated boost converter in secondary rectifier. *IEEE Trans Power Electron* 2017;32:8237–42.
- [62] Zhifu W, Yupu W, Yinan R. Design of closed-loop control system for a bidirectional full bridge DC/DC converter. *Appl Energy* 2017;194:617–25.
- [63] Surapaneni RK, Yelaverthi DB, Rathore AK. Cycloconverter-based double-ended microinverter topologies for solar photovoltaic AC module. *IEEE J Emerg Sel Top Power Electron* 2016;4:1354–61.
- [64] Asad R, Shoulaie A. Determination, simulation and implementation of a novel improved industrial cycloconverter. *Int Trans Electr Energy Syst* 2013;23:166–80.
- [65] Liu Y, Heydt GT, Chu RF. The power quality impact of cycloconverter control strategies. *IEEE Trans Power Deliv* 2005;20:1711–8.
- [66] Wheeler PW, Rodriguez J, Clare JC, Empringham L, Weinstein A. Matrix converters: a technology review. *IEEE Trans Ind Electron* 2002;49:276–88.
- [67] Hannan MA, Ali JA, Mohamed A, Hussain A. Optimization techniques to enhance the performance of induction motor drives: A review. *Renew Sustain Energy Rev* 2017;81:1611–26.
- [68] Sathishkumar H, Parthasarathy SS. A novel neuro-fuzzy controller for vector controlled induction motor drive. *Energy Procedia* 2017;138:698–703.
- [69] Dettori S, Iannino V, Colla V, Signorini A. An adaptive Fuzzy logic-based approach to PID control of steam turbines in solar applications. *Appl Energy* 2018;227:655–64.
- [70] Francis R, Chidambaram IA. Optimized PI+ load-frequency controller using BWNN approach for an interconnected reheat power system with RFB and hydrogen electrolyser units. *Int J Electr Power Energy Syst* 2015;67:381–92.
- [71] Choi HH, Yun HM, Kim Y. Implementation of Evolutionary Fuzzy PID Speed Controller for PM Synchronous Motor. *IEEE Trans Ind Informatics* 2015;11:540–7.
- [72] HongboZou Li H. Tuning of PI-PD controller using extended non-minimal state space model predictive control for the stabilized gasoline vapor pressure in a stabilized tower. *Chemom Intell Lab Syst* 2015;142:1–8.
- [73] Zhong J, Li L. Tuning fractional-order PID controllers for a solid-core magnetic bearing system. *IEEE Trans Control Syst Technol* 2015;23:1648–56.
- [74] Daful AG. Comparative study of PID tuning methods for processes with large & small delay times. 2018 Adv. Sci. Eng. Technol. Int. Conf., IEEE; 2018, p. 1–7.
- [75] Hoque MM, Hannan MA, Mohamed A. Charging and discharging model of lithium-ion battery for charge equalization control using particle swarm optimization algorithm. *J Renew Sustain Energy* 2016;8:065701.

- [76] Rashid MH. Power Electronics Handbook, 4th Edition; 2017.
- [77] Singh P, Dwivedi P. Integration of new evolutionary approach with artificial neural network for solving short term load forecast problem. *Appl Energy* 2018;217:537–49.
- [78] Rashid MH. Power electronics handbook: devices, circuits, and applications. Butterworth-Heinemann; 2011.
- [79] Lipu MSH, Hannan MA, Hussain A. Feature selection and optimal neural network algorithm for the state of charge estimation of lithium-ion battery for electric vehicle application. *Int J Renew Energy Res* 2017;7:1700–8.
- [80] Lipu MSH, Hannan MA, Hussain A, Saad MHM, Ayob A, Blaabjerg F. State of charge estimation for lithium-ion battery using recurrent NARX neural network model based lightning search algorithm. *IEEE Access* 2018;6:28150–61.
- [81] Keshitkar A, Arzanpour S. An adaptive fuzzy logic system for residential energy management in smart grid environments. *Appl Energy* 2017;186:68–81.
- [82] Lekhchine S, Bahi T, Soufi Y. Indirect rotor field oriented control based on fuzzy logic controlled double star induction machine. *Int J Electr Power Energy Syst* 2014;57:206–11.
- [83] Ali JA, Hannan MA, Mohamed A, Abdolrasol MGM. Fuzzy logic speed controller optimization approach for induction motor drive using backtracking search algorithm. *Measurement* 2016;78:49–62.
- [84] Cheng P-C, Peng B-R, Liu Y-H, Cheng Y-S, Huang J-W. Optimization of a Fuzzy-Logic-Control-Based MPPT Algorithm Using the Particle Swarm Optimization Technique. *Energies* 2015;8:5338–60.
- [85] Yang L, Entchev E. Performance prediction of a hybrid microgeneration system using Adaptive Neuro-Fuzzy Inference System (ANFIS) technique. *Appl Energy* 2014;134:197–203.
- [86] Denai MA, Attia SA. Intelligent control of an induction motor. *Electr Power Components Syst* 2002;30:409–27.
- [87] Yang H, Fu Y, Wang D. Multi-ANFIS model based synchronous tracking control of high-speed electric multiple unit. *IEEE Trans Fuzzy Syst* 2018;26:1472–84.
- [88] Jang J-SR. ANFIS: adaptive-network-based fuzzy inference system. *IEEE Trans Syst Man Cybern* 1993;23:665–85.
- [89] Falahati S, Taher SA, Shahidehpour M. Grid frequency control with electric vehicles by using of an optimized fuzzy controller. *Appl Energy* 2016;178:918–28.
- [90] Jolfaei MG, Sharaf AM, Shariatmadar SM, Poudeh MB. A hybrid PSS–SSSC GA-stabilization scheme for damping power system small signal oscillations. *Int J Electr Power Energy Syst* 2016;75:337–44.
- [91] Kanwar N, Gupta N, Niazi KR, Swarnkar A, Bansal RC. Simultaneous allocation of distributed energy resource using improved particle swarm optimization. *Appl Energy* 2017;185:1684–93.
- [92] Rashedi E, Nezamabadi-pour H, Saryazdi S. GSA: A Gravitational Search Algorithm. *Inf Sci (Ny)* 2009;179:2232–48.
- [93] Civicioglu P. Backtracking Search Optimization Algorithm for numerical optimization problems; 2013.
- [94] Shareef H, Ibrahim AA, Mutlag AH. Lightning search algorithm. *Appl. Soft Comput* 2015;36:315–33.
- [95] Wang D, Luo H, Grunder O, Lin Y, Guo H. Multi-step ahead electricity price forecasting using a hybrid model based on two-layer decomposition technique and BP neural network optimized by firefly algorithm. *Appl Energy* 2017;190:390–407.
- [96] Yilmaz S, Küçükşille EU. A new modification approach on bat algorithm for solving optimization problems. *Appl Soft Comput* 2015;28:259–75.
- [97] Kumar V, Chhabra JK, Kumar D. Differential Search Algorithm for Multiobjective Problems. *Procedia Comput Sci* 2015;48:22–8.
- [98] Lipu MSH, Karim TF. Energy efficiency opportunities and savings potential for electric motor and its impact on GHG emissions reduction. *Int J Electr Comput Eng* 2013;3.
- [99] Rodriguez Ponce R, Talavera DV. FPGA implementation of decimal division for motor control drives. *IEEE Lat Am Trans* 2016;14:3980–5.
- [100] Wang G, Yang R, Xu D. DSP-based control of sensorless IPMSM drives for wide-speed-range operation. *IEEE Trans Ind Electron* 2013;60:720–7.
- [101] Hannan MA, Ali JA, Ker PJ, Mohamed A, Lipu MSH, Hussain A. Switching techniques and intelligent controllers for induction motor drive: issues and recommendations. *IEEE Access* 2018;6:47489–510.
- [102] Hannan MA, Ali JA, Hussain A, Hasim FH, Amirulddin UAU, Uddin MN, et al. A quantum lightning search algorithm-based fuzzy speed controller for induction motor drive. *IEEE Access* 2018;6:1214–23.
- [103] Hannan MA, Ali JA, Mohamed A, Amirulddin UAU, Tan NML, Uddin MN. Quantum-behaved lightning search algorithm to improve indirect field-oriented fuzzy-PI control for IM drive. In: 2017 IEEE Ind. Appl. Soc. Annu. Meet., IEEE; 2017, p. 1–8.
- [104] Sun Xiang-Dong, Koh Kang-Hoon, Byung-Gyu Yu, Matsui M. Fuzzy-Logic-Based V/f Control of an Induction Motor for a DC Grid Power-Leveling System Using Flywheel Energy Storage Equipment. *IEEE Trans Ind Electron* 2009;56:3161–8.
- [105] Raza S, Larabi A, Barazane L, Manceur M, Essounbouli N, Hamzaoui A. Implementation of a new fuzzy vector control of induction motor. *ISA Trans* 2014;53:744–54.
- [106] Gdaim S, Mtibaa A, Mimouni MF. Design and Experimental Implementation of DTC of an Induction Machine Based on Fuzzy Logic Control on FPGA. *IEEE Trans Fuzzy Syst* 2015;23:644–55.
- [107] Bounar N, Boulkroune A, Boudjema F, M'Saad M, Farza M. Adaptive fuzzy vector control for a doubly-fed induction motor. *Neurocomputing* 2015;151:756–69.
- [108] Nathenas TG, Adamidis GA. A new approach for SVPWM of a three level inverter-induction motor fed-neutral point balancing algorithm. In: *Int Aegean Conf Electr Mach Power Electron Electromotion, Jt Conf, IEEE; 2011, p. 221–6.*
- [109] Verma A, Sarangi S, Kolekar MH. Stator winding fault prediction of induction motors using multiscale entropy and grey fuzzy optimization methods. *Comput Electr Eng* 2014;40:2246–58.
- [110] Chekkal S, Lahaçani NA, Aouzellag D, Ghedamsi K. Fuzzy logic control strategy of wind generator based on the dual-stator induction generator. *Int J Electr Power Energy Syst* 2014;59:166–75.
- [111] Paicu MC, Boldea I, Andreescu G-D, Blaabjerg F. Very low speed performance of active flux based sensorless control: interior permanent magnet synchronous motor vector control versus direct torque and flux control. *IET Electr Power Appl* 2009;3:551.
- [112] Velusami S, Singaravelu S. Steady state modeling and fuzzy logic based analysis of wind driven single phase induction generators. *Renew Energy* 2007;32:2386–406.
- [113] El-Barbary ZMS. Fuzzy logic based controller for five-phase induction motor drive system. *Alexandria Eng J* 2012;51:263–8.
- [114] Wang S-Y, Tseng C-L, Chiu C-J. Design of a novel adaptive TSK-fuzzy speed controller for use in direct torque control induction motor drives. *Appl Soft Comput* 2015;31:396–404.
- [115] Zhan L, Zhou K. Field-programmable Gate Array Based Fuzzy Sliding-mode Controller for a Permanent Magnet Synchronous Motor Drive. *Electr Power Components Syst* 2014;42:1440–51.
- [116] Cheng P-J, Cheng C-H, Tung C-C. Design of DC motor's torque control using DSP. *J Inf Optim Sci* 2009;30:1197–207.
- [117] Masiala M, Vafakhah B, Salmon J, Knight A. Fuzzy self-tuning speed control of an indirect field-oriented control induction motor drive. In: 2007 IEEE Ind Appl Annu Meet, IEEE; 2007, p. 1008–14.
- [118] Zhang Yongchang, Zhu Jianguo, Zhao Zhengming, Wei Xu, An Dorrell DG. Improved direct torque control for three-level inverter-fed induction motor sensorless drive. *IEEE Trans Power Electron* 2012;27:1502–13.
- [119] Bird IG, Zelaya De La Parra H. Fuzzy logic torque ripple reduction for DTC based AC drives. *Electron Lett* 1997;33:1501.
- [120] Uddin MN, Radwan TS, Rahman MA. Performances of novel fuzzy logic based indirect vector control for induction motor drive. In: *Conf Rec 2000 IEEE Ind Appl Conf Thirty-Fifth IAS Annu Meet World Conf Ind Appl Electr Energy (Cat. No. 00CH37129)*, vol. 2, IEEE, p. 1225–31.
- [121] Bizon N. Energy efficiency of multiport power converters used in plug-in/V2G fuel cell vehicles. *Appl Energy* 2012;96:431–43.
- [122] Zou Y, Hu X, Ma H, Li SE. Combined State of Charge and State of Health estimation over lithium-ion battery cell cycle lifespan for electric vehicles. *J Power Sources* 2015;273:793–803.
- [123] Hoque MM, Hannan MA, Mohamed A. Optimal algorithms for the charge equalisation controller of series connected lithium-ion battery cells in electric vehicle applications. *IET Electr Syst Transp* 2017;7:267–77.
- [124] Hoque MM, Hannan MA, Mohamed A. Voltage equalization control algorithm for monitoring and balancing of series connected lithium-ion battery. *J Renew Sustain Energy* 2016;8:025703.
- [125] Baronti F, Roncella R, Saletti R. Performance comparison of active balancing techniques for lithium-ion batteries. *J Power Sources* 2014;267:603–9.
- [126] Kim CH, Kim MY, Moon GW. A modularized charge equalizer using a battery monitoring ic for series-connected li-ion battery strings in electric vehicles. *IEEE Trans Power Electron* 2013;28:3779–87.
- [127] Lambert SM, Pickert V, Atkinson DJ, Zhan H. Transformer-based equalization circuit applied to n-number of high capacitance cells. *IEEE Trans Power Electron* 2016;31:1334–43.
- [128] Kim MY, Kim CH, Kim JH, Moon GW. A chain structure of switched capacitor for improved cell balancing speed of lithium-ion batteries. *IEEE Trans Ind Electron* 2014;61:3989–99.
- [129] Li S, Mi CC, Zhang M. A high-efficiency active battery-balancing circuit using multiwinding transformer. *IEEE Trans Ind Appl* 2013;49:198–207.
- [130] Uno M, Kukita A. Single-switch single-transformer cell voltage equalizer based on forward-flyback resonant inverter and voltage multiplier for series-connected energy storage cells. *IEEE Trans Veh Technol* 2014;63:4232–47.
- [131] Uno M, Kukita A. Bidirectional PWM converter integrating cell voltage equalizer using series-resonant voltage multiplier for series-connected energy storage cells. *IEEE Trans Power Electron* 2015;30:3077–90.
- [132] Hannan M, Hoque M, Ker P, Begum R, Mohamed A. Charge equalization controller algorithm for series-connected lithium-ion battery storage systems: modeling and applications. *Energies* 2017;10:1390.
- [133] Hannan MA, Hoque MM, Peng S, Uddin MN. Lithium-ion battery charge equalization algorithm for electric vehicle applications. *IEEE Trans Ind Appl* 2017;53:2541–9.
- [134] Park Hong-Sun, Kim Chong-Eun, Kim Chol-Ho, Moon Gun-Woo, Lee Joong-Hui. A modularized charge equalizer for an HEV lithium-ion battery string. *IEEE Trans Ind Electron* 2009;56:1464–76.
- [135] Cui N, Ji X, Yu G, Zhang C. Modularized charge equalizer using fuzzy logic controller for Lithium-ion battery system. In: 2015 IEEE Int Telecommun Energy Conf, IEEE; 2015, p. 1–5.
- [136] Yan J, Cheng Z, Xu G, Qian H, Xu Y. Fuzzy control for battery equalization based on state of charge. In: 2010 IEEE 72nd Veh Technol Conf - Fall, IEEE; 2010, p. 1–7.
- [137] Huang W, Abu Qahouq JA. Energy sharing control scheme for state-of-charge balancing of distributed battery energy storage system. *IEEE Trans Ind Electron* 2015;62:2764–76.
- [138] Yang D, Li S, Qi G. A bidirectional flyback cell equalizer for series-connected lithium iron phosphate batteries. In: 2015 6th Int Conf Power Electron Syst Appl, IEEE; 2015, p. 1–5.
- [139] Lin F-J, Lu K-C, Yang B-H. Recurrent fuzzy cerebellar model articulation neural network based power control of a single-stage three-phase grid-connected photovoltaic system during grid faults. *IEEE Trans Ind Electron* 2017;64:1258–68.

- [140] Kumar N, Hussain I, Singh B, Panigrahi BK. Implementation of multilayer fifth-order generalized integrator-based adaptive control for grid-tied solar PV energy conversion system. *IEEE Trans Ind Informatics* 2018;14:2857–68.
- [141] Rahimi R, Farhangi S, Farhangi B, Moradi GR, Afshari E, Blaabjerg F. H8 inverter to reduce leakage current in transformerless three-phase grid-connected photovoltaic systems. *IEEE J Emerg Sel Top Power Electron* 2018;6:910–8.
- [142] Saravanan S, Ramesh Babu N. Analysis and implementation of high step-up DC-DC converter for PV based grid application. *Appl Energy* 2017;190:64–72.
- [143] Rodriguez P, Citro C, Candela JI, Rocabert J, Luna A. Flexible Grid Connection and Islanding of SPC-Based PV Power Converters. *IEEE Trans Ind Appl* 2018;54:2690–702.
- [144] Wang Y, Wang F. Novel three-phase three-level-stacked neutral point clamped grid-tied solar inverter with a split phase controller. *IEEE Trans Power Electron* 2013;28:2856–66.
- [145] Mahela OP, Shaik AG. Comprehensive overview of grid interfaced solar photovoltaic systems. *Renew Sustain Energy Rev* 2017;68:316–32.
- [146] Dutta S, Chatterjee K. A Buck and boost based grid connected PV inverter maximizing power yield from two PV arrays in mismatched environmental conditions. *IEEE Trans Ind Electron* 2018;65:5561–71.
- [147] Basaran K, Cetin NS, Borekci S. Energy management for on-grid and off-grid wind/PV and battery hybrid systems. *IET Renew Power Gener* 2017;11:642–9.
- [148] Sangwongwanich A, Yang Y, Blaabjerg F. High-performance constant power generation in grid-connected PV systems. *IEEE Trans Power Electron* 2016;31:1822–5.
- [149] Errouissi R, Al-Durra A, Mueen SM. A robust continuous-time MPC of a DC-DC boost converter interfaced with a grid-connected photovoltaic system. *IEEE J Photovolt* 2016;6:1619–29.
- [150] Mahmud N, Zahedi A, Mahmud A. A cooperative operation of novel PV inverter control scheme and storage energy management system based on ANFIS for voltage regulation of grid-tied PV system. *IEEE Trans Ind Inform* 2017;13:2657–68.
- [151] Rong F, Gong X, Huang S. A novel grid-connected PV system based on MMC to get the maximum power under partial shading conditions. *IEEE Trans Power Electron* 2017;32:4320–33.
- [152] Sangwongwanich A, Yang Y, Blaabjerg F. A sensorless power reserve control strategy for two-stage grid-connected PV systems. *IEEE Trans Power Electron* 2017;32:8559–69.
- [153] Zhu Y, Fei J. Adaptive global fast terminal sliding mode control of grid-connected photovoltaic system using fuzzy neural network approach. *IEEE Access* 2017;5:9476–84.
- [154] Dutta S, Debnath D, Chatterjee K. A grid-connected single-phase transformerless inverter controlling two solar PV arrays operating under different atmospheric conditions. *IEEE Trans Ind Electron* 2018;65:374–85.
- [155] Islam MR, Guo Y, Zhu J. A high-frequency link multilevel cascaded medium-voltage converter for direct grid integration of renewable energy systems. *IEEE Trans Power Electron* 2014;29:4167–82.
- [156] Shahbazi M, Poure P, Saadate S, Zolghadri MR. Five-leg converter topology for wind energy conversion system with doubly fed induction generator. *Renew Energy* 2011;36:3187–94.
- [157] Islam MR, Guo Y, Zhu J. Power converters for wind turbines: Current and future development. *Mater Process Energy Commun Curr Res Technol Dev* 2013;559–71.
- [158] Marugán AP, Márquez FPG, Perez JMP, Ruiz-Hernández D. A survey of artificial neural network in wind energy systems. *Appl Energy* 2018;228:1822–36.
- [159] Naidu NKS, Singh B. Grid-interfaced DFIG-based variable speed wind energy conversion system with power smoothing. *IEEE Trans Sustain Energy* 2017;8:51–8.
- [160] Soliman MA, Hasanien HM, Azazi HZ, El-kholly EE, Mahmoud SA. Hybrid ANFIS-GA-based control scheme for performance enhancement of a grid-connected wind generator. *IET Renew Power Gener* 2018;12:832–43.
- [161] Mondal S, Kastha D. Maximum active and reactive power capability of a matrix converter-fed DFIG-based wind energy conversion system. *IEEE J Emerg Sel Top Power Electron* 2017;5:1322–33.
- [162] Xiong L, Wang J, Mi X, Khan MW. Fractional order sliding mode based direct power control of grid-connected DFIG. *IEEE Trans Power Syst* 2018;33:3087–96.
- [163] Chowdhury MA, Mahmud MA, Shen W, Pota HR. Nonlinear controller design for series-compensated DFIG-based wind farms to mitigate subsynchronous control interaction. *IEEE Trans Energy Convers* 2017;32:707–19.
- [164] Hu J, Yuan H, Yuan X. Modeling of DFIG-based WTs for small-signal stability analysis in DVC timescale in power electrified power systems. *IEEE Trans Energy Convers* 2017;32:1151–65.
- [165] Song Y, Blaabjerg F, Wang X. Analysis and active damping of multiple high frequency resonances in DFIG system. *IEEE Trans Energy Convers* 2017;32:369–81.
- [166] Yang B, Hu Y, Huang H, Shu H, Yu T, Jiang L. Perturbation estimation based robust state feedback control for grid connected DFIG wind energy conversion system. *Int J Hydrogen Energy* 2017;42:20994–1005.
- [167] Rahimi M. Improvement of energy conversion efficiency and damping of wind turbine response in grid connected DFIG based wind turbines. *Int J Electr Power Energy Syst* 2018;95:11–25.
- [168] Shukla RD, Tripathi RK, Thakur P. DC grid/bus tied DFIG based wind energy system. *Renew Energy* 2017;108:179–93.
- [169] Zhang XS, Yu T, Pan ZN, Yang B, Bao T. Lifelong learning for complementary generation control of interconnected power grids with high-penetration renewables and EVs. *IEEE Trans Power Syst* 2018;33:4097–110.
- [170] Liu B, Zhuo F, Zhu Y, Yi H. System operation and energy management of a renewable energy-based DC micro-grid for high penetration depth application. *IEEE Trans Smart Grid* 2015;6:1147–55.
- [171] Liu Y-W, Rau S-H, Wu C-J, Lee W-J. Improvement of power quality by using advanced reactive power compensation. *IEEE Trans Ind Appl* 2018;54:18–24.
- [172] Dong H, Yuan S, Han Z, Ding X, Ma S, Han X. A comprehensive strategy for power quality improvement of multi-inverter-based microgrid with mixed loads. *IEEE Access* 2018;6:30903–16.
- [173] Khederzadeh M, Ghorbani A. Impact of VSC-based multiline FACTS controllers on distance protection of transmission lines. *IEEE Trans Power Deliv* 2012;27:32–9.
- [174] Hannan MA, Islam NN, Mohamed A, Lipu MSH, Ker PJ, Rashid MM, Shareef H. Artificial intelligent based damping controller optimization for the multi-machine power system: a review. *IEEE Access* 2018;39574–94.
- [175] Lipu MSH, Karim TF. Effectiveness of FACTS controllers and HVDC transmissions for improving power system stability and increasing power transmission capability. *Int J Energy Power Eng* 2013;2:154.
- [176] Mahela OP, Shaik AG. A review of distribution static compensator. *Renew Sustain Energy Rev* 2015;50:531–46.
- [177] Kalair A, Abas N, Khan N. Comparative study of HVAC and HVDC transmission systems. *Renew Sustain Energy Rev* 2016;59:1653–75.
- [178] Mosaad SAA, Issa UH, Hassan MS. Risks affecting the delivery of HVAC systems: Identifying and analysis. *J Build Eng* 2018;16:20–30.
- [179] Liu L, Liu C. VSCs-HVDC may improve the Electrical Grid Architecture in future world. *Renew Sustain Energy Rev* 2016;62:1162–70.
- [180] Sau-Bassols J, Prieto-Araujo E, Galceran-Arellano S, Gomis-Bellmunt O. Operation and control of a Current Source Converter series tapping of an LCC-HVDC link for integration of Offshore Wind Power Plants. *Electr Power Syst Res* 2016;141:510–21.
- [181] Korompili A, Wu Q, Zhao H. Review of VSC HVDC connection for offshore wind power integration. *Renew Sustain Energy Rev* 2016;59:1405–14.
- [182] Shen L, Tang Q, Li T, Wang Y, Song F. A review on VSC-HVDC reliability modeling and evaluation techniques. *IOP Conf Ser Mater Sci Eng* 2017;199:012133.
- [183] Shah R, Sánchez JC, Preece R, Barnes M. Stability and control of mixed AC-DC systems with VSC-HVDC: a review. *IET Gener Transm Distrib* 2018;12:2207–19.
- [184] You H, Cai X. Stepped two-level operation of nonisolated modular DC/DC converter applied in high-voltage DC grid. *IEEE J Emerg Sel Top Power Electron* 2018;6:1540–52.
- [185] González-Torres I, Miranda-Vidales H, Espinoza J, Méndez-Barrios C-F, González M. State feedback control assisted by a gain scheduling scheme for three-level NPC VSC-HVDC transmission systems. *Electr Power Syst Res* 2018;157:227–37.
- [186] Mahmoudi H, Aleenejad M, Ahmadi R. Modulated model predictive control of modular multilevel converters in VSC-HVDC systems. *IEEE Trans Power Deliv* 2017;1–11.
- [187] Hannan MA, Hussain I, Ker PJ, Hoque MM, Hossain Lipu MS, Hussain A, et al. Advanced control strategies of VSC Based HVDC transmission system: Issues and potential recommendations. *IEEE Access* 2018;6:78352–69.
- [188] Mohan N, Undeland TM, Robbins WP. Power electronics: converters, applications, and design. John Wiley & Sons; 2003.
- [189] Shinoda K, Benchaib A, Dai J, Guillaud X. DC voltage control of MMC-based HVDC grid with Virtual Capacitor Control. In: 2017 19th Eur Conf Power Electron Appl (EPE'17 ECCE Eur. IEEE; 2017, p. P.1-P.10.
- [190] Feldman R, Tomasini M, Amankwah E, Clare JC, Wheeler PW, Trainer DR, et al. A hybrid modular multilevel voltage source converter for HVDC power transmission. *IEEE Trans Ind Appl* 2013;49:1577–88.
- [191] Khazaei J, Idowu P, Asrari A, Shafaye A, Piyasinghe L. Review of HVDC control in weak AC grids. *Electr Power Syst Res* 2018;162:194–206.
- [192] Sun H, Du L, Liang G. Calculation of electromagnetic radiation of VSC-HVDC converter system. *IEEE Trans Magn* 2016;52:1–4.
- [193] Castro LM, Acha E. A unified modeling approach of multi-terminal VSC-HVDC links for dynamic simulations of large-scale power systems. *IEEE Trans Power Syst* 2016;31:5051–60.
- [194] Zhang M, Yuan X, Hu J. Inertia and primary frequency provisions of PLL-synchronized VSC HVDC when attached to islanded AC system. *IEEE Trans Power Syst* 2018;33:4179–88.
- [195] Moawwad A, El Moursi MS, Xiao W. Advanced fault ride-through management scheme for VSC-HVDC connecting offshore wind farms. *IEEE Trans Power Syst* 2016;31:4923–34.
- [196] Li H, Liu C, Li G, Irvani R. An enhanced DC voltage droop-control for the VSC-HVDC grid. *IEEE Trans Power Syst* 2017;32:1520–7.
- [197] Wang W, Barnes M, Marjanovic O, Cwikowski O. Impact of DC breaker systems on multiterminal VSC-HVDC stability. *IEEE Trans Power Deliv* 2016;31:769–79.
- [198] Li B, Jing F, Jia J, Li B. Research on saturated iron-core superconductive fault current limiters applied in VSC-HVDC systems. *IEEE Trans Appl Supercond* 2016;26:1–5.
- [199] Safari Tirtashi MR, Samuelsson O, Svensson J. Impedance matching for VSC-HVDC and energy storage damping controllers. *IEEE Trans Power Deliv* 2017;1–11.
- [200] Adeyi OD, Cheah-Mane M, Liang J, Jenkins N. Fast frequency response from offshore multiterminal VSC-HVDC schemes. *IEEE Trans Power Deliv* 2017;32:2442–52.
- [201] Renedo J, Garcia-Cerrada A, Rouco L. Reactive-power coordination in VSC-HVDC multi-terminal systems for transient stability improvement. *IEEE Trans Power Syst* 2017;32:3758–67.
- [202] Raza A, Akhtar A, Jamil M, Abbas G, Gilani SO, Yuchao L, et al. A protection scheme for multi-terminal VSC-HVDC transmission systems. *IEEE Access* 2018;6:3159–66.
- [203] Abdelwahed MA, El-Saadany EF. Power sharing control strategy of multiterminal VSC-HVDC transmission systems utilizing adaptive voltage droop. *IEEE Trans Sustain Energy* 2017;8:605–15.
- [204] Wang H, Cao J, He Z, Yang J, Han Z, Chen G. Research on overvoltage for XLPE cable in a modular multilevel converter HVDC transmission system. *IEEE Trans*

- Power Deliv 2016;31:683–92.
- [205] Raza M, Prieto-Araujo E, Gomis-Bellmunt O. Small-signal stability analysis of offshore AC network having multiple VSC-HVDC systems. *IEEE Trans Power Deliv* 2018;33:830–9.
- [206] Nanou SI, Papathanassiou SA. Grid code compatibility of VSC-HVDC connected offshore wind turbines employing power synchronization control. *IEEE Trans Power Syst* 2016;31:5042–50.
- [207] Molina MG. Energy storage and power electronics technologies: a strong combination to empower the transformation to the smart grid. *Proc IEEE* 2017;105:2191–219.
- [208] Liu S, Wang X, Liu PX. A stochastic stability enhancement method of grid-connected distributed energy storage systems. *IEEE Trans Smart Grid* 2017;8:2062–70.
- [209] Ghosh S, Kamalasan S. An energy function-based optimal control strategy for output stabilization of integrated DFIG-flywheel energy storage system. *IEEE Trans Smart Grid* 2017;8:1922–31.
- [210] Pahlevani M, Eren S, Guerrero JM, Jain P. A hybrid estimator for active/reactive power control of single-phase distributed generation systems with energy storage. *IEEE Trans Power Electron* 2016;31:2919–36.
- [211] Eren S, Pahlevani M, Bakhshai A, Jain P. A digital current control technique for grid-connected AC/DC converters used for energy storage systems. *IEEE Trans Power Electron* 2017;32:3970–88.
- [212] Grover-Silva E, Agoua XG, Girard R, Karinotakis G. Stochastic multi-temporal optimal power flow approach for the management of grid-connected storage. *CIREN - Open Access Proc J* 2017;2017:2011–4.
- [213] Arcos-Aviles D, Pascual J, Marroyo L, Sanchis P, Guinjoan F. Fuzzy logic-based energy management system design for residential grid-connected microgrids. *IEEE Trans Smart Grid* 2018;9:530–43.
- [214] Chatziniakolaou E, Rogers DJ. A comparison of grid-connected battery energy storage system designs. *IEEE Trans Power Electron* 2017;32:6913–23.
- [215] Ross M, Abbey C, Bouffard F, Joos G. Microgrid economic dispatch with energy storage systems. *IEEE Trans Smart Grid* 2018;9:3039–47.
- [216] Sun S, Liang B, Dong M, Taylor JA. Phase balancing using energy storage in power grids under uncertainty. *IEEE Trans Power Syst* 2016;31:3891–903.
- [217] Luo X, Lee CK, Ng WM, Yan S, Chaudhuri B, Hui SYR. Use of adaptive thermal storage system as smart load for voltage control and demand response. *IEEE Trans Smart Grid* 2017;8:1231–41.
- [218] Dong J, Gao F, Guan X, Zhai Q, Wu J. Storage-reserve sizing with qualified reliability for connected high renewable penetration micro-grid. *IEEE Trans Sustain Energy* 2016;7:732–43.
- [219] Papadopoulos PN, Guo T, Milanovic JV. Probabilistic framework for online identification of dynamic behavior of power systems with renewable generation. *IEEE Trans Power Syst* 2018;33:45–54.
- [220] Lipu MSH, Hussain A, Saad MHM, Ayob A, Hannan MA. Improved recurrent NARX neural network model for state of charge estimation of lithium-ion battery using pso algorithm. In: 2018 IEEE Symp Comput Appl Ind Electron. IEEE; 2018, p. 354–9.
- [221] Lee KT, Dai MJ, Chuang CC. Temperature-compensated model for lithium-ion polymer batteries with extended Kalman filter state-of-charge estimation for an implantable charger. *IEEE Trans Ind Electron* 2018;65:589–96.
- [222] Lipu MSH, Hussain A, Saad MHM, Hannan MA. Optimal neural network approach for estimating state of energy of lithium-ion battery using heuristic optimization techniques. In: 2017 6th Int Conf Electr Eng Informatics. IEEE; 2017, p. 1–6.
- [223] Altin N, Sefa İ. dSPACE based adaptive neuro-fuzzy controller of grid interactive inverter. *Energy Convers Manage* 2012;56:130–9.
- [224] Teng L-T, Hung Y-C, Lin F-J, Chen C-Y. FPGA-based adaptive backstepping control system using RBFN for linear induction motor drive. *IET Electr Power Appl* 2008;2:325–40.